Journal of Plant Physiology 257 (2021) 153341

Contents lists available at ScienceDirect

Journal of Plant Physiology

journal homepage: www.elsevier.com/locate/jplph

Humboldt Review

Plasmodesmata and the problems with size: Interpreting the confusion

Winfried S. Peters [a,b], Kaare H. Jensen [c], Howard A. Stone [d], Michael Knoblauch [a,*]

[a] School of Biological Sciences, Washington State University, Pullman, WA, 99164, USA
[b] Department of Biology, Purdue University Fort Wayne, Fort Wayne, IN, 46805, USA
[c] Department of Physics, Technical University of Denmark, DK-2800 Kgs., Lyngby, Denmark
[d] Department of Mechanical and Aerospace Engineering, Princeton University, Princeton, NJ, 08544, USA

ARTICLE INFO

Keywords:
Cell theory
Electron microscopy
Microfluidics
Nanofluidics
Plasmodesma
Symplasm

ABSTRACT

Plant tissues exhibit a symplasmic organization; the individual protoplasts are connected to their neighbors via cytoplasmic bridges that extend through pores in the cell walls. These bridges may have diameters of a micrometer or more, as in the sieve pores of the phloem, but in most cell types they are smaller. Historically, botanists referred to cytoplasmic bridges of all sizes as plasmodesmata. The meaning of the term began to shift when the transmission electron microscope (TEM) became the preferred tool for studying these structures. Today, a plasmodesma is widely understood to be a 'nano-scale' pore. Unfortunately, our understanding of these nanoscopic channels suffers from methodological limitations. This is exemplified by the fact that state-of-the-art EM techniques appear to reveal plasmodesmal pore structures that are much smaller than the tracer molecules known to diffuse through these pores. In general, transport processes in pores that have dimensions in the size range of the transported molecules are governed by different physical parameters than transport process in the macroscopic realm. This can lead to unexpected effects, as experience in nanofluidic technologies demonstrates. Our discussion of problems of size in plasmodesma research leads us to conclude that the field will benefit from technomimetic reasoning – the utilization of concepts developed in applied nanofluidics for the interpretation of biological systems.

1. Introduction

1.1. Cell-to-cell links in multicellular organisms

Cells in multicellular organisms coordinate their activities and cooperate in ways that are developmentally and physiologically meaningful on the organismal level (Kay and Smith, 1989; Hancock, 2005; Lim et al., 2015). The necessary transfer of information may occur through signaling molecules exchanged between neighboring cells like in neuronal synapses, or, as in the case of hormones, over distances well above the size of the cells involved. However, communication among neighboring cells or cell groups often is accomplished more directly. Physical connections may establish various degrees of cytoplasmic continuity, ranging from symplasmic plant tissues in which every cell is linked to its neighbors through narrow cytoplasmic bridges, to multinuclear syncytia and coenobia that lack any structural cellularization altogether (Robards et al., 1990; Płachno and Świątek, 2011; Bloemendal and Kück, 2013).

Animal cells lack cell walls, and intercellular electrical and biochemical coupling is achieved by gap junctions, short proteinaceous channels that connect the plasma membranes of adjacent cells (Goldberg et al., 2004; Meşe et al., 2007; Cervera et al., 2018). Intriguingly, gap junctions are structurally and functionally similar in chordates and non-chordates, but are assembled from apparently non-homologous proteins in the two groups (Skerrett and Williams, 2017). Animal cells also may form thin, membrane-covered filopodia by actin polymerization. Various structures of this type have been described under different names, and some have been implied to be involved in cell-to-cell signaling (Kornberg and Roy, 2014a). One version referred to as a tunneling nanotube provides symplasmic pathways for the exchange of material up to the size of mitochondria between cells (Abounit and Zurzolo, 2012; Sisakhtnezhad and Khosravi, 2015; Rustom, 2016). Another version, the cytonemes, were described first in *Drosophila* (Ramírez-Weber and Kornberg, 1999) and are important for the exchange of various developmental signals (Zhang and Scholpp, 2019). However, the underlying mechanisms do not seem to require

* Corresponding author at: 100 Dairy Road, Eastlick Hall G81, Washington State University, Pullman, 99164, USA.
E-mail addresses: petersw@pfw.edu (W.S. Peters), khjensen@fysik.dtu.dk (K.H. Jensen), hastone@princeton.edu (H.A. Stone), knoblauch@wsu.edu (M. Knoblauch).

https://doi.org/10.1016/j.jplph.2020.153341
Received 20 November 2020; Received in revised form 4 December 2020; Accepted 7 December 2020
Available online 16 December 2020

cytoplasmic continuity between cells, as the cells linked by cytonemes may rather form so-called morphogenetic synapses (González-Méndez et al., 2019).

Cytoplasmic bridges between the wall-covered cells of fungi, algae, and plants are more stable structures because they require more or less permanent openings in the rigid cell walls. The walls that separate hyphal cells in fungi often are perforated by septal pores (Markham, 1994; Dhavale and Jedd, 2007). Septal pores can be relatively large compared to the diameter of the cells, allowing for cytoplasmic bulk flow and even the movement of organelles along the hyphae (Lew, 2005). However, much smaller cytoplasmic bridges with diameters of a few tens of nanometers have also been reported in certain fungal cells (Marchant, 1976). An even larger variety of cytoplasmic connections occurs in photoautotrophs with walled cells, which include the major taxa of algae and land plants (Raven, 2005). These structures are the topic of the present review.

1.2. Cytoplasmic bridges in plants

Cytoplasmic cell-to-cell links in vascular plants range in size from sieve pores that can have diameters in excess of 5 µm (Mullendore et al., 2010) to much narrower channels of 50 nm diameter or less (Ehlers and Kollmann, 2001). Nano-scale links today are referred to as plasmodesmata (singular: plasmodesma). However, explicit definitions of the term *plasmodesma* are quite ambiguous in both the historical and modern literature. In order to discuss this ambiguity and its conceptual implications, we first have to summarize essential features of plasmodesma morphology, development, and function.

From a developmental viewpoint, we can distinguish primary and secondary plasmodesmata (Fig. 1A, B). Primary plasmodesmata originate during cell division, as the formation of the cell plate remains incomplete due to the presence of strands of endoplasmic reticulum (ER) that traverse the plane in which the plate assembles (Hepler, 1982). As a result, not only the cytosol with the plasma membrane but also the desmotubule, a tube of ER membrane, typically extend through these pores. Secondary plasmodesmata form in existing cell walls between neighboring cells, but the mechanisms by which the location of these new cytoplasmic bridges is determined, the cell wall is degraded locally, and the desmotubule connects the ER of the two cells remain poorly understood (Falkner et al., 2008; Ehlers and van Bel, 2010). Plasmodesmata may differentiate into a variety of differently structured cell-to-cell bridges (Ehlers and Kollmann, 2001; Yan and Liu, 2020).

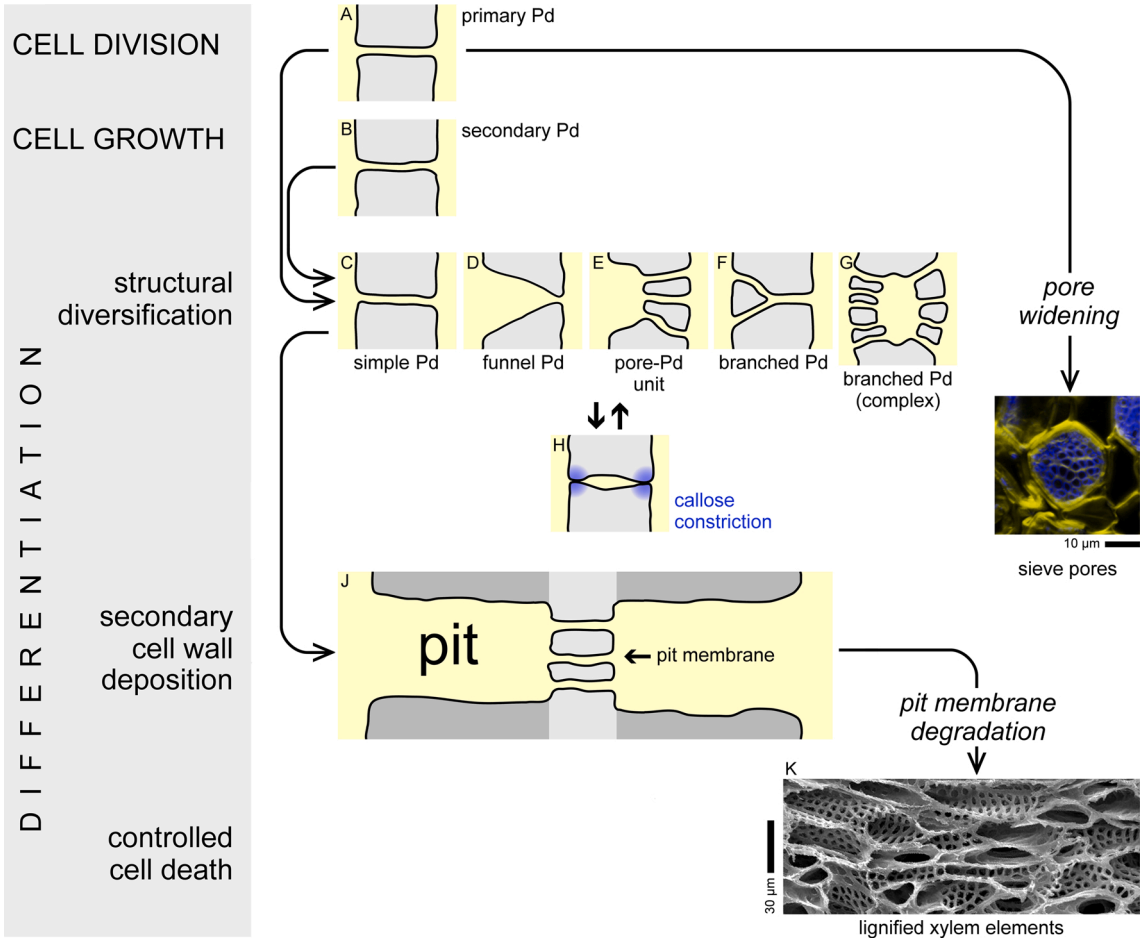

Fig. 1. Cytoplasmic communications between plant cells and their developmental relationships. In the sketches, desmotubules are omitted for clarity (cytoplasm, yellow; cell walls, gray; plasma membrane, black lines). Plasmodesmata (Pd) form in cell division (A; primary Pd) or at a later stage (B; these secondary plasmodesmata may be branched at the time they develop). When a cell approaches functional maturity, simple plasmodesmata (C) may transform into derived structures such as funnel plasmodesmata (D), pore-plasmodesma units (E), or branched plasmodesmata (F), which may be complex (G) with or without central cavity. Plasmodesmal pores of all types can be constricted reversibly by callose deposition (H; blue). In young sieve elements, plasmodesmata widen to give rise to sieve pores (I; fluorescence micrograph of a sieve plate in *Gerrardanthus macrorhizus*. Blue, callose; yellow, cellulose). In cells producing secondary wall layers (J; dark gray), corresponding pairs of pits may develop in which the persisting primary wall (light gray) with plasmodesmata forms a pit membrane. Pit membrane degradation in dying xylem elements establishes open wall pits for water transport (K; scanning electron micrograph of empty, perforated cell walls in the xylem of *Cucurbita maxima*). We emphasize that the figure presents a necessarily simplified view of the gamut of structures and the underlying developmental dynamics that have been observed in plants.

Simple plasmodesmata (Fig. 1C) are cylindrical cell wall pores found in numerous tissues, whereas funnel plasmodesmata (Fig. 1D) appear restricted to certain cell types in phloem unloading zones (Ross-Elliott et al., 2017). In the walls between sieve elements and companion cells, characteristic pore-plasmodesma units (Fig. 1E) with a large pore facing the sieve element and several narrower channels on the side of the companion cell are found (Esau and Thorsch, 1985). More or less complex systems of branching channels (Fig. 1F, G) may develop from simple plasmodesmata by diverse mechanisms (Kollmann and Glockmann, 1999). All structural variants of plasmodesmata may be constricted or closed temporarily or permanently by localized deposition of the cell wall polysaccharide, callose (Fig. 1H; Zavaliev et al., 2011). Local cell wall degradation leading to a widening of plasmodesmata gives rise to large sieve pores in young sieve elements (Fig. 1I; Esau and Thorsch, 1985). When cells deposit layers of secondary wall on their primary walls, some areas of the primary wall with plasmodesmata are left unoccluded. The primary wall thus becomes a so-called pit membrane, and the plasmodesmata become part of a larger cytoplasmic bridge between two cells, consisting of a pair of corresponding pits in the secondary walls and the pit membrane on which the pits converge (Fig. 1J; Evert, 2006, pp. 74–76). Developing xylem elements synthesize lignified secondary walls with large pits. When these cells initiate controlled cell death, they degrade some pit membranes, resulting in open pits in the empty secondary cell walls that function in the long-distance transport of water (Fig. 1K; Esau and Charvat, 1978).

General descriptions of plasmodesmata often include a desmotubule as a characteristic component (Ding et al., 1999; Lucas and Lee, 2004; Lee et al., 2011). However, not all cytoplasmic bridges between walled cells possess desmotubules, for example the plasmodesmata in some multicellular algae (Cook and Graham, 1999; Raven, 2005). The sieve pores of angiosperms generally lack desmotubules (Evert, 1990; Eleftheriou, 1990) while those of conifers (Schulz, 1990) and other basal tracheophytes (Behnke, 1990) contain ER loops at least occasionally. The ER appears involved in certain plasmodesmal transport processes in higher plants (Grabski et al., 1993; Martens et al., 2006; Barton et al., 2011; Spiegelman et al., 2019) including the movement of viral pathogens (Heinlein, 2015; Pitzalis and Heinlein, 2017). An obvious consequence of the presence of a desmotubule is the restriction of the cross-sectional area of the cytosolic space in the plasmodesma. In these cases, only a cytosolic sleeve, the space between the desmotubule and the inner surface of the plasma membrane, is available for the cell-to-cell movement of cytosolic components (the frequently used term ‘cytoplasmic sleeve’ is potentially misleading as the ER and thus the desmotubule is part of the cytoplasm by definition). Ultrastructural data appear to suggest that proteins tether desmotubules to the plasma membrane (Ding et al., 1992). Such linkers obviously further constrict the cytosolic path.

The functional significance of intercellular cytoplasmic bridges lies in the provision of pathways for the symplasmic movement of materials. Plants utilize these pathways for the distribution of metabolites, in particular the long-distance translocation of photoassimilates in sieve tubes that relies on the symplasmic continuity established by the large sieve pores (Münch, 1930; Knoblauch and Peters, 2013). Moreover, much narrower plasmodesmata also provide regulated routes for the exchange of a variety of specific biochemical signals (Schulz, 1999; Burch-Smith and Zambryski, 2012; Tilsner et al., 2016) including proteins, which may diffuse through the pores (non-targeted transport) or utilize specific mechanisms that in effect widen the plasmodesmatal aperture (targeted transport; Crawford and Zambryski, 2001). The targeted transport of transcription factors, for example, has essential functions in the coordinated development and differentiation of cells and tissues in vascular plants (Jackson, 2005; Wu and Gallagher, 2011; Otero et al., 2016). The permeability of some plasmodesmata for comparatively large protein molecules can be visualized directly by the cell-to-cell movement of fluorescent tracer proteins such as GFP, which has a molecular mass of 27 kDa (Imlau et al., 1999; Stadler et al., 2005). However, no generalized conclusion concerning the so-called size exclusion limit (size of the largest particle that can pass through a pore) of plasmodesmal pores can be drawn from this fact. For example, consider the polymer trap mechanism applied by some of the plant species that load sugars into their sieve tube system via symplasmic routes (McCaskill and Turgeon, 2007; Rennie and Turgeon, 2009). According to this model, sucrose (342 Da) moves via plasmodesmata into intermediary cells, where it is transformed into the oligosaccharides raffinose (504 Da) and stachyose (666 Da). The larger size of these oligosaccharides prevents their diffusion through the plasmodesmata through which sucrose enters, resulting in an accumulation of total sugars in the intermediary cells. The physics of plasmodesmal transport in these cells is more complex than it may appear at first sight (Comtet et al., 2017), but in any case one has to conclude that the plasmodesmata in question are readily permeable for molecules of under about 400–500 Da while the movement of molecules of larger sizes is inhibited. Proteins like GFP, which has 40 times the molecular weight of stachyose, cannot be expected to pass through these channels. Thus it seems evident that plasmodesmal efficient pore sizes differ drastically depending on cell type, physiological status, or developmental stage (Oparka et al., 1999; Schulz, 1999; Rutschow et al., 2011).

A special case of symplasmic cell-to-cell transport is the movement of ions, which could transmit fluctuations of the electrical membrane potential along arrays of cytoplasmically continuous cells. Long-range electrical signaling in specific cases such as the ‘sensitive plant’, *Mimosa pudica*, has been demonstrated over a century ago (e.g., Bose, 1926), and the symplasmic sieve tube network appears to provide the required low-resistance route for the propagation of plant action potentials and other types of electrical waves (Fromm and Lautner, 2007; Choi et al., 2016). It should be noted, though, that electrical coupling does not necessarily imply communication in the sense of an exchange of physiologically meaningful signals between cells (Taiz et al., 2019). Neither does electrical signaling depend on cytoplasmic bridges between cells. After all, most animal nervous systems process electrically encoded information without cytoplasmic continuity among the neurons involved.

Despite all progress, a closer look at current plasmodesma research reveals surprising inconsistencies. For example, Nicolas et al. (2017) applied state-of-the-art techniques of electron microscopy to cells that had been shown to readily exchange fluorescent proteins via symplasmic pathways, and found that the plasmodesmata between these cells lacked cytosolic sleeves altogether. Thus, our most advanced imaging methodologies combined with unambiguous physiological observations appear to suggest that macromolecules of significant size can move through channels that do not even seem to exist. Something clearly is wrong. We suspect that misconceptions concerning, first, the production of images of very small biological objects and how to ‘read’ them, and second, the physical concepts we utilize, or fail to utilize to understand the workings of very small pores and channels might be to blame. This review presents some thoughts on problems of size. Because questions of size played important roles in the development of ideas about what plasmodesmata actually are, we first will discuss the apparent discovery of plasmodesmata in the late 19th century.

2. What is a plasmodesma, actually?

2.1. Historical confusion

2.1.1. Original definition(s)

European scientists generally read Latin and classical Greek as recently as a century ago, and terms like πλάσμα (*plasma*; anything formed or molded, body) and δεσμός (*desmos*; any means of binding, bond) could be expected to be understood when used casually. In the heated controversy about the morphogenesis of the nervous system that raged in the early 20th century (Billings, 1971), animal anatomists writing in German, English, and French applied derivatives of

plasmodesma to cell extensions and intercellular bridges that they assumed to be involved in the development of nerves, apparently without seeing a need to formally define or explain the term (e.g., Held, 1906; Ramón Cajal, 1908; Neal, 1921). At about the same time, Eduard Strasburger (1844–1912) suggested *plasmodesma* to denote 'the threads of plasm that traverse the plant cell walls, and thus elevate the single protoplasts to an aggregate organism' ('die Plasmafäden, welche die pflanzlichen Zellwände durchsetzen und damit die einzelnen Protoplasten zu einem Gesammtorganismus erheben'; Strasburger, 1901, p. 503). The word plasmodesma has been botanical jargon ever since, but its meaning went through several metamorphoses and remained strangely vague at all times.

Strasburger's original definition of *plasmodesma* had two components. A descriptive statement about the structures to which he referred ('threads of plasm that traverse the plant cell walls') was followed by a statement of the implication of the existence of these structures for the relationship between cells and organism ('elevate the single protoplasts to an aggregate organism'). With regard to the structural component of Strasburger's definition, we wish to highlight three points. First, Strasburger obviously could not consider desmotubules in the context of his definition since the organelle that became known as the endoplasmic reticulum was recognized only half a century later (Schuldiner and Schwappach, 2013). Second, fungi and algae counted as plants at the time, so that, for instance, the septal pores of fungi qualified as plasmodesmata. In fact, septal pores, which had been demonstrated to allow for cytoplasmic bulk flow along hyphae (Ternetz, 1900) at the time Strasburger suggested the term, were referred to as plasmodesmata by Ernst Münch (1876–1946) when he presented his pressure flow hypothesis of phloem transport in 1930 (p. 211; Knoblauch and Peters, 2017). Third, Strasburger's definition included no explicit size limits. As a result, scientists adopting Strasburger's definition as it stood usually considered sieve pores plasmodesmata. This explains why Baker (1952), in his comprehensive analysis of the history of the cell theory, argued that the first botanist to ever have seen plasmodesmata was Theodor Hartig (1805–1880). Hartig had described a novel type of vessel characterized by porous cross walls or sieve plates in 1837 (compare Fig. 4B below). Baker's view was not uncommon; Münch, for instance, used the terms 'sieve pores' ('Siebporen') and 'plasmodesmata of sieve tubes' ('Plasmodesmen der Siebröhren') synonymously (1930, pp. 59–60). Interestingly, separated from the definition of plasmodesma by some 40 pages of text, Strasburger discussed the possibility of a size-dependent functional difference between wide openings such as sieve pores and plasmodesmata that were smaller (Strasburger, 1901, pp. 544-545). A decade earlier, Strasburger had postulated that the cytoplasm had two major components, the kinoplasm and the trophoplasm (Strasburger, 1892, 1893). The details of this hypothesis and its modifications over the years do not need to concern us here. What is important in our context is that in 1901, Strasburger thought, first, that the kinoplasm itself did not move (although it seemed responsible for the movement of other components of the cell), and second, that the outermost periphery of each protoplast consisted of a thin layer of kinoplasm. From this he concluded that perforations of the cell wall with diameters up to the thickness of the 'kinoplasmatic skin layer' were probably filled with kinoplasm only, making 'mass movements' through these narrow channels unlikely (Fig. 2A). In contrast, larger openings such as sieve pores, which had peripheral layers of kinoplasm but were filled mostly with trophoplasm, allowed for mass flow between cells (Fig. 2B). The kinoplasm-trophoplasm hypothesis never met with general acceptance, which may explain why Strasburger's reasoning about possible functional differences between wide and narrow cell connections never developed into a formal definition of different categories of pores.

In the second part of the definition of *plasmodesma*, Strasburger (1901) apparently referred to the organismic concept, the idea that the living plant was a coherent unit partitioned into cooperating compartments, as opposed to the cell-theoretical dogma that portrayed multicellular organisms as assemblages of essentially independent entities,

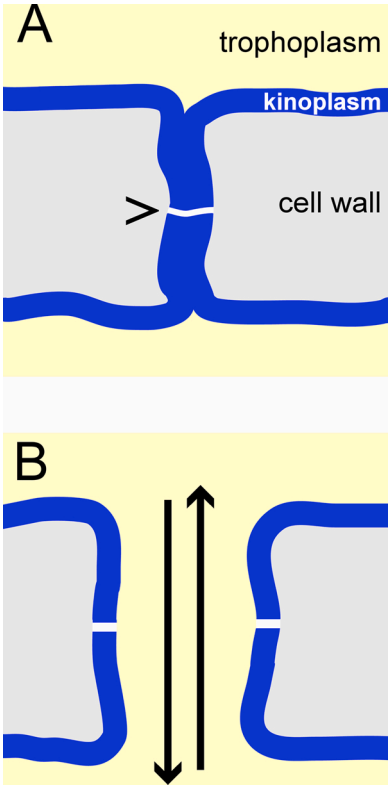

Fig. 2. Schematic representations of narrow (A) and wide (B) cytoplasmic bridges between cells, as they were discussed by Eduard Strasburger (1901) in the publication in which he introduced the term *plasmodesma* into the plant sciences. At the time, Strasburger assumed that the cytoplasm consisted of a relatively immobile portion he termed kinoplasm (blue) and a more fluid portion he called trophoplasm (yellow). The kinoplasm formed thin peripheral layers covering the cell walls (gray). Cell wall pores of diameters about as large as the kinoplasm's thickness were filled with kinoplasm only, preventing any mass transport between the cells (A). Strasburger assumed that the two threads of kinoplasm in narrow pores (A) were in close contact but did not merge (arrowhead in A points to the contact zone); narrow plasmodesmata therefore did not establish a symplasmic organization of the tissue. In contrast, larger channels (B) such as sieve pores could be filled partially with trophoplasm or non-cytoplasmic materials such as 'slime', allowing for symplasmic mass flow (arrows) through the pore. Despite the differences Strasburger hypothesized to exist between narrow and wide pores, both qualified as *plasmodesmata* according to the formal definition he presented.

the cells (for a discussion of the historical and theoretical context, see Reynolds, 2018; for shorter overviews, see Nicholson, 2010; Reynolds, 2010). Somewhat simplified, the difference on a conceptual level is that in the first case, the whole organism represents an autonomous actor that determines the limits of cellular independence, whereas in the second case, the organism is but the result of the autonomous activities of a large number of 'elementary organisms'. Strasburger's definition of plasmodesmata appears in line with the organismic interpretation as it suggested that the plant became a unit by virtue of the physical links between the cells. It would be incorrect, though, to conclude that Strasburger's plasmodesmata established a symplasmic organization of the plant body. Pointing to the limitations of contemporary microscopy, Strasburger (1901, p. 591) emphasized that 'it cannot be decided whether the threads of plasm, which traverse the wall without visible interruption, are really continuous or only in close contact at their tips'. Nonetheless he tentatively concluded that the 'morphological coherence in a multicellular plant organism is not based on the mixing of the substance of the plasmodesmata, but only on their intimate association' (Strasburger, 1901, p. 595). In other words, Strasburger thought that plant cells connected to their neighbors not by establishing symplasmic

continuity, but by sending out pairs of plasmodesmata – one from each cell – that contacted each other without merging in the middle of the cell wall (Fig. 2A). It should be clear that Eduard Strasburger, famed for introducing the term plasmodesma into plant science, did not mean anything like the structures we call plasmodesmata today when he used that word. Structurally, Strasburger's narrow plasmodesmata (Fig. 2A) more closely resemble modern models of chemical synapses in nervous systems (Kandel et al., 2012) and morphogenetic synapses in embryos (Kornberg and Roy, 2014b).

2.1.2. *Sieve plates and the 'discovery' of plasmodesmata*

The historical development of the empirical basis of Strasburger's definition of the term *plasmodesma* was summarized by the British botanist William Hillhouse (1850–1910), who worked with Strasburger at the time, as follows: 'The existence of an open communication between certain cells of higher plants, namely between the different elements which compose sieve tubes, has been known for many years. Our knowledge of these structural relationships, which began with the great work of Hartig … has now much expanded through the investigations of distinguished botanists like von Mohl, Nägeli, Hanstein, de Bary, and Dippel, and most recently of Wilhelm, Janczewski, and Russow. … In the year 1879, Tangl found another group of examples for the continuity of the protoplasm in endosperm cells of seeds of *Strychnos nux-vomica*, *Areca oleraceae*, and *Phoenix dactylifera*' (Hillhouse, 1883, pp. 89-90; our translation from the original German). Quite obviously, Hillhouse considered the Austrian botanist Eduard Tangl (1848–1905) a notable contributor among many, but was far from ascribing a paradigm-changing breakthrough to him. In remarkable contrast, modern authors are celebrating Tangl as the 'discoverer of plasmodesmata' (Köhler and Carr, 2006), who through this discovery 'launched the visionary concept that cell-cell communication integrates the functioning of plant tissues' (van Bel and Oparka, 1995, p. 174; for similar statements, see e.g. Meeuse, 1957; Carr, 1976; Roberts, 2005; Kehr and Kragler, 2018; van Bel, 2018). But what did Eduard Tangl himself think?

In his often-cited paper that actually was published first in 1880, Tangl repeatedly emphasized the similarity between the intercellular 'open communications' he saw in the endosperm of certain palms on one hand and the long-known sieve plates in the phloem on the other. He finally concluded that what he saw in the endosperm was 'parenchyma tissue equipped with sieve plates' ('mit Siebplatten ausgestattete Parenchymgewebe'; Tangl, 1880, p. 187). The analogy was not merely structural. As Tangl explained, because the endosperm cell walls resembled sieve plates so closely, these walls probably also functioned like sieve plates. In most species, the endosperm is a storage tissue in the seeds that provides materials and energy to germinating plant embryos (Vijayaraghavan and Prabhakar, 1984). Tangl hypothesized that the sieve plates in the walls of endosperm cells facilitated the import of material into the developing seed as well as the rapid release of these materials during germination by enabling symplasmic mass fluxes from cell to cell (Tangl, 1880, pp. 187-188). In other words, Tangl built on available knowledge about the symplasmic structure of sieve tubes and extended this concept to the endosperm of certain palms. He reported that 'open communications' were present only in specific cell layers of the endosperm but not in other cells. Moreover, Tangl stressed that such communications did not seem to exist at all in the endosperm of several of the species that he had studied. Consequently, he emphasized that he

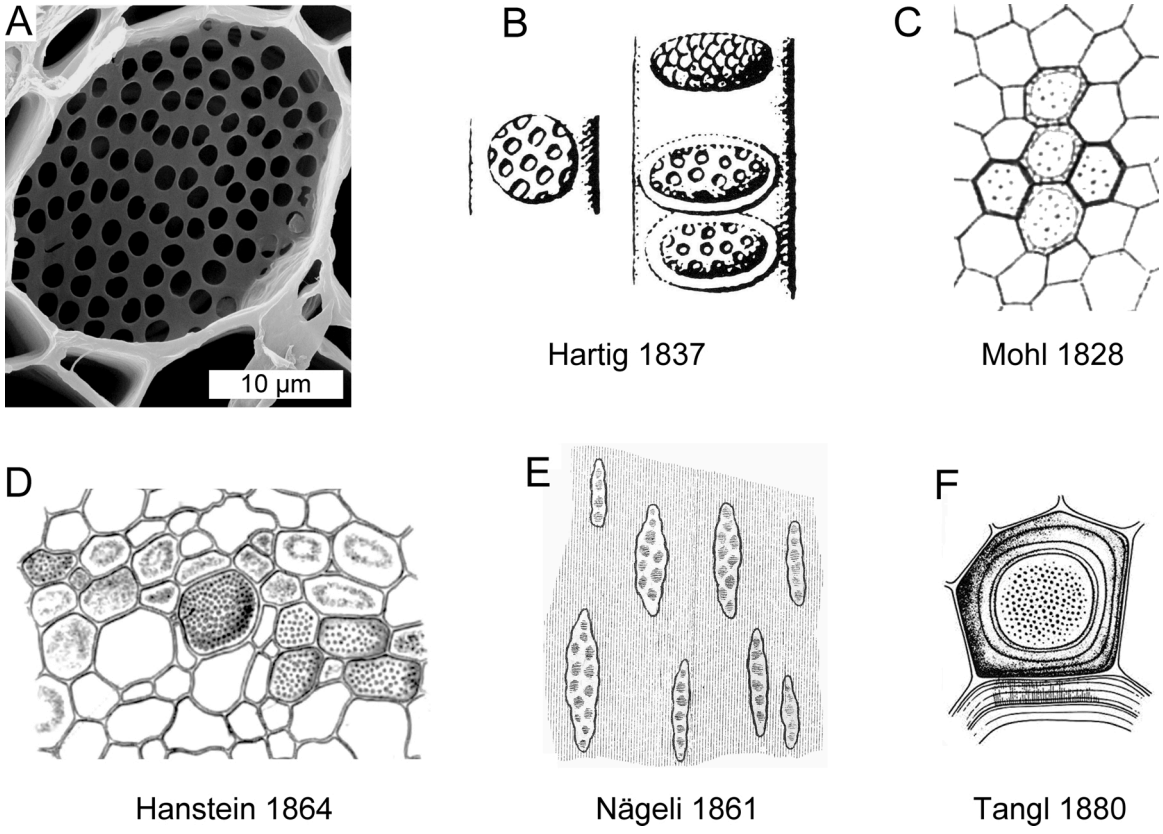

Fig. 3. Images of cell wall pores in plants that in the interpretation of their authors enabled the transport of cell contents from cell to cell. The direction of view is onto the surface of the cell walls of interest in all images, showing the pores as dots or more or less circular openings in the plane of the wall. A, scanning electronmicrograph of a sieve plate between two sieve elements in the bamboo, *Phyllostachys nuda*. B, drawings of sieve plates of various tree species, from the earliest description of these structures (Hartig, 1837; Figs. 41 and 42 on Table I). C, parenchymatic cells in the pith of internodes of *Hoya carnosa*, some of them with porous, thickened walls (Mohl, 1828; part of Fig. 35 on Table IV). D, several sieve tubes with sieve plates in an internode of *Ricinus communis*, embedded in undifferentiated parenchyma cells (Hanstein, 1864; part of Fig. 2 on Table IV). E, eight clusters of 'sieve pores' in the wall of a cortical parenchyma cell, from an internode of *Cucurbita pepo* (Nägeli, 1861; Fig. 44 on Table II). F, endosperm cell in the seed of *Strychnos nux-vomica* with thickened, sieve plate-like walls (Tangl, 1880; Fig. 12 on Table V).

had no basis for broad generalizations of his findings (Tangl, 1880, p. 188).

With a steadily expanding variety of plant tissues in which cytoplasmic cell-to-cell bridges had been discovered, the idea that 'sieve tubes with their long-known connecting strands [of cytoplasm] represent only a special case in which the strands are particularly thick and thus easily visible' (Kienitz-Gerloff, 1891, p. 34) became widely accepted by the turn of the century. Our Fig. 3 presents a visual summary of selected findings that helped pave the way toward Strasburger's usage of the term plasmodesma. Sieve plates, such as the example shown in the SEM micrograph (Fig. 3A), played an essential role in the development of the concept of a symplasm. The first description of sieve plates in the phloem came from Theodor Hartig (1837; Fig. 3B). However, cell wall pits ('Tüpfel') that corresponded between neighboring parenchyma cells had been characterized a decade earlier by Hugo Mohl (1828), who expressed no doubts that these structures functioned in the transport of materials from cell to cell (Fig. 3C). In the 1860s, the symplasmic nature of sieve tubes had been demonstrated independently by several researchers; our example (Fig. 3D) shows the sieve elements of *Ricinus communis* studied by Johannes Hanstein (1864). To our knowledge, the first application of the term 'sieve plates' to structures in the walls of parenchymatic cells outside the vasculature was by Nägeli (1861; Fig. 3E), predating the analogous conclusion by Eduard Tangl by two decades. Finally, we have chosen a drawing of an endosperm cell from Tangl (1880) that seems to explain particularly well why this author concluded that these cells were 'equipped with sieve plates' (Fig. 3F). We conclude that while the history of the symplasm concept certainly deserves more detailed analyses, it is evident that the currently popular narrative of Eduard Tangl, the discoverer of plasmodesmata, is a myth that reflects our notorious fascination with 'the great heroes of an earlier age' (Kuhn, 1996, pp. 136-143) rather than historical reality.

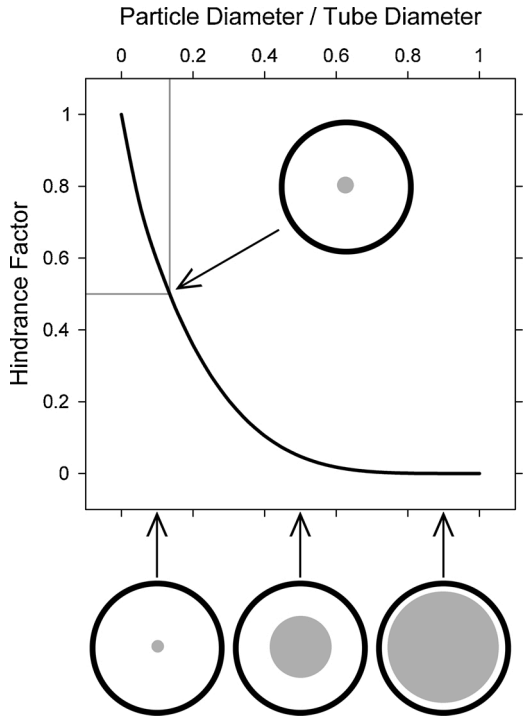

Fig. 4. The diffusional hindrance factor for a spherical particle diffusing in a cylindrical pore plotted as a function of the ratio between the particle and the tube (pore) diameter, redrawn from Dechadilok and Deen (2006; Fig. 2 and eq. 16). Some diameter ratios are visualized as grey fields (diffusing particles) in black circles (cross-sections of the pore). The diameter ratio at which the diffusivity of the particle is reduced by 50 % compared to its diffusivity in unconfined space is highlighted in the graph.

2.2. Modern ambiguities

As we have seen, Strasburger (1901) had provided a broad definition of the term plasmodesma that included a wide range of cytoplasmic connections between cells, with plasmodesmata of different sizes facilitating distinct types of interaction, and only the largest channels establishing a symplasmic organization of tissues (Fig. 2). Unfortunately, we expose our students to a similarly confusing situation. If they consult the glossaries of modern textbooks of plant science to find out what a plasmodesma is, they will retrieve definitions that appear in agreement with Strasburger's original wording, for instance:

> '**plasmodesma**, *pl.* **plasmodesmata** [Gk. *plasma*, form, + *desma*, bond]: The minute cytoplasmic threads that extend through openings in cell walls and connect the protoplasts of adjacent living cells.' (Raven et al., 1999, p. 906)

Based on this statement (we could list dozens of equivalent examples), the students will have to conclude that septal pores in fungi are plasmodesmata, and that the same holds for cell wall pits as well as sieve pores in sieve plates; after all, the holes in sieve plates are 'pores through which the protoplasts of adjacent sieve elements are interconnected' (Raven et al., 1999, p. 909). Occasionally one finds applications of the term *plasmodesma* in this wide, Strasburgerian sense in the primary literature. For example, Yan and Liu (2020, p. 2510) subsumed funnel plasmodesmata, pore-plasmodesma units, and sieve pores under 'various forms of plasmodesmata'. However, most working plant biologists including ourselves would refrain from calling sieve pores plasmodesmata – but why, exactly?

Pore geometry might play a role. Scientists in micro- and nanofluidics sometimes define *pores* as openings in which length is commensurable with radius, whereas in *channels*, length is much larger than radius (e.g., Tagliazucchi and Szleifer, 2015, p. 131). Although plant cell biologists do not seem to generally apply this definition, plasmodesmata are much longer than wide in schematic drawings in textbooks and the primary literature, while this is not so for sieve pores. Sometimes versions of Strasburger's reasoning about the significance of pore sizes seem to be adopted, for example when plasmodesmata are introduced as 'nanoscopic canals' (Nicolas et al., 2018). However, cytoplasmic bridges with diameters in the µm range such as sieve pores develop from primary plasmodesmata that are smaller than 50 nm in diameter (Fig. 1). This prompts the question at exactly what size a widening plasmodesma turns into a different type of channel – and what this means, if anything. An early attempt to explicitly define 'true plasmodesmata' came from Meeuse (1957, p. 6), who presented a definition that was equivalent to Strasburger's original one cited above, and then added: 'they are never so wide as to permit a real fusion of protoplasts or migration of protoplasmic inclusions, such as nuclei, plastids, microsomes, granula, under normal conditions, but may be converted into wider protoplasmic connections or, conversely, arise in special cases by a reduction in diameter of wider protoplasm strands connecting adjacent cells'. This argument resembles Strasburger's assessment of the nature of small plasmodesmata (Fig. 2A): if true plasmodesmata are too small to permit a 'real fusion of protoplasts', they do not, by definition, establish a symplasmic organization of tissues. However, an inconsistency of this definition surfaced when Meeuse (1957, p. 19) stated that the occasionally observed 'nucleus migration' was a 'possible argument in favor of the protoplasmic nature of the plasmodesmata'. One wonders how this could be, given that plasmodesmata were defined as pores not wide enough to allow for such migration.

2.3. Size matters, but not alone

Employing size as a defining criterion for functionally meaningful categories of pores or channels easily becomes confusing if these

openings widen or shrink depending on the cell's developmental state and physiological needs (Fig. 1). What adds to the problem is that different physical parameters control material flow in channels of different sizes, and that size is not the only factor that determines in which situations the flow regime changes. To clarify the fact, consider the technologically important switch between turbulent and laminar fluid flow in a tube. Under certain conditions, the fluid moves in laminar layers that do not mix, and the flow velocity varies from zero at the tube walls (this condition is referred to as 'no slip' of the fluid) to maximum in the tube's center; the profile of fluid velocities across the tube diameter is parabolic and stable over time. In other situations, the velocity distribution fluctuates vigorously in space and time, and the fluid mixes as it moves; this is turbulent flow. Physical and chemical processes in channels or pipes in which fluids move in laminar flow do not follow the intuitive rules based on our experience with turbulent flow that dominates in the macroscopic world (Vogel, 1994), and we exploit this by various microfluidics and lab-on-a-chip technologies (Beebe et al., 2002; Velve-Casquillas et al., 2010; Zhong et al., 2019).

But exactly when does the switch between the turbulent and laminar flow regimes occur? This depends on a dimensionless parameter, the Reynolds number (*Re*). *Re* can be computed from the density (ρ), dynamic viscosity (μ), and velocity (*v*) of the moving fluid, and a characteristic linear dimension (*L*) of the structure in or around which the fluid flows (Falkovich, 2018):

$$\mathrm{Re} = \frac{\mathrm{v}\,\rho\,\mathrm{L}}{\mu} \quad (1)$$

The inclusion of *L*, the characteristic dimension, shows that size plays an important role in determining the flow regime, but only in the context of the other parameters in this equation (Squires and Quake, 2005). At constant flow velocity in a cylindrical tube (where *L* is the tube diameter), the transition from laminar flow (low *Re*) to turbulent flow (high *Re*) may occur when the tube diameter widens; at constant tube diameter, however, the same transition may occur when flow velocity increases. To complicate matters, temperature changes also may trigger the transition, if fluid density and viscosity are temperature-dependent. As a consequence, size alone is insufficient to predict flow characteristics in a given structure with certainty, which we will have to keep in mind when analyzing plasmodesma structure.

2.4. A technomimetic approach

Like similarly sized channels in artificial microfluidics systems, sieve elements transporting photoassimilate solutions have low Reynolds numbers (generally, $Re < 1$), implying that flow in sieve tubes is laminar (Jensen et al., 2012). In fact, artificial sieve tubes for studying processes that occur in their natural counterparts can be manufactured by standard methods for the production of technological microfluidics devices (Knoblauch et al., 2012). *Re* values for sieve pores are in the same general range but somewhat lower than those of the sieve elements connected by the sieve pores (Jensen et al., 2012). However, when channel dimensions become much smaller than those of typical sieve pores, physical parameters gain controlling influence on the transport process that remain negligible in microfluidics or larger systems (Schoch et al., 2008; Bocquet and Charlaix, 2010; Haywood et al., 2015). In this context it seems noteworthy that the International Union of Pure and Applied Chemistry (IUPAC) recommended distinguishing three types of pores in order 'to clarify … the selection of appropriate experimental techniques for the characterization of porous materials' and 'the appraisal and significance of experimental data' (Rouquerol et al., 1994, p. 1741). These categories of pores that have to be characterized by different practical approaches are broadly defined by their sizes. The IUPAC recommendation distinguishes between micropores (width or diameter under about 2 nm), mesopores (about 2–50 nm), and macropores (exceeding about 50 nm; Rouquerol et al., 1994). This terminology may seem unusual. In many contexts, size classes are defined by the appropriate units of measurement. For example, microfluidics deals with processes in structures with sizes in the micrometer range, nanofluidics with structures in the nanometer range, etc. In contrast, the IUPAC terminology does not refer to units of measurement. Rather, it is to be understood literally: micropores are just small pores, mesopores are intermediate pores, and macropores are large ones. What distinguishes them are not different units of size measurement, but the different physical parameters that are most relevant for realistic descriptions of the transport processes that may occur within the pores (Verweij et al., 2007). The size limits set by the IUPAC classification must not be taken to be strictly fixed, and the effects of parameters other than size require careful evaluation in every real case. Nonetheless, the two transitions that separate the three categories of pores correspond to relevant physical phenomena.

The size limit between meso- and micropores (at around 2 nm) roughly coincides with the transition from the continuum to the subcontinuum realm (Corry et al., 2000; Holt et al., 2006; Thomas and McGaughey, 2009; Bruno et al., 2018). The continuum assumptions of the diffusion/advection theories successfully applied to transport phenomena at larger scales break down in this range. Fluids and fluid components cannot be treated as continua in micropores (in the IUPAC definition of the term), and have to be analyzed by particle-based models that evaluate movement in terms of molecular interactions (Bocquet and Charlaix, 2010).

The size limit between meso- and macropores, on the other hand, can be interpreted as the transition from transport processes that are accurately quantified only when interactions between channel walls and moving molecules are taken into account (mesopores), to conditions in which such interactions have negligible influence on the overall process (macropores; compare Verweij et al., 2007). A well-studied example is the steric hindrance of diffusion that occurs when the size of a particle approaches the width of the pore in which it diffuses (Dechadilok and Deen, 2006). The effect can be quantified as the diffusional hindrance factor, *H*, which represents the diffusivity of a particle in a given confinement relative to its diffusivity in unconfined space. The dependence of *H* on the ratio between the diameter of a spherical particle and the diameter of a cylindrical tube that contains the particle is shown in Fig. 4 (compare eq. 16 and Fig. 2 in Dechadilok and Deen, 2006). This analysis suggests that the bulk diffusivity of a particle with diameter *D* is halved when it is confined in a tube of about 7 *D* diameter.

The quantification of steric hindrance of diffusion (Fig. 4) considers geometry but no other factors. However, electrostatic forces acting between electrically charged pore walls and ions in the transported fluid are an important category of wall-fluid interactions (Plecis et al., 2005; Schoch et al., 2008). The charged surface of the walls attracts counter-ions while repelling co-ions, which will lead to the formation of a so-called electrical double layer. If the physiological conditions are such that the electrical double layer is comparable to or larger than the dimensiones of the tube, then double layer effects will control the behavior of ions across the tube's entire cross-section. In this case, the pore will be permselective: the movement of counterions in the pore will be facilitated whereas the entry of co-ions into the pore will be inhibited. As an interesting consequence, asymmetric nanopores can act as current rectifiers and ion-selective conductors due to their geometry alone (Cervera et al., 2006; Singh, 2016; Hsu et al., 2018, 2019). Double layer thickness increases with increasing charge density on the surface of the pore's wall. In materials used for the production of artificial nanochannels, charge densities on fully ionized surfaces can reach 0.3 $\mathrm{C\,m^{-2}}$ (Schoch et al., 2008), but typical values are fractions thereof (e.g., Tajparast et al., 2015; Hsu et al., 2018; Ramirez et al., 2019). Because counter-ions accumulating on the wall surface shield the charges in the wall, the thickness of the double layer also decreases with increasing ionic strength of the solution. This effect can be quantified by the Debye length, which, to give an example, is about 1 nm for a 0.1 M KCl solution (McLaughlin, 1989). Only when the Debye length is negligible compared to the radius of a transporting tube, can ions move freely in

the bulk phase and double layer effects can be ignored when describing pressure or voltage-driven ion movement along the tube (Tagliazucchi and Szleifer, 2015).

Throughout their history, the life sciences have benefitted from technomimetic reasoning, the transfer of concepts developed in the context of crafts and technologies to biological systems (Knoblauch and Peters, 2004). The development of nanofluidics technologies seems more likely to provide fundamental insights into the physical basis of transport processes in meso- and micropores as defined by IUPAC than the study of similarly sized biological channels, simply because experimental conditions are so much easier controlled when studying the former. Intriguingly, published widths of apparently transporting plasmodesmata or, if they have a desmotubule, those of their cytosolic sleeves cover a range from literally zero (Nicolas et al., 2017) to several tens, even hundreds of nanometers (Robards, 1976). Practical experience reflected by the IUPAC categories of nano-scale pores should alarm us to the fact that all these cell-to-cell bridges are not just differently sized versions of the same thing. They rather fall into distinct categories as far as the physical nature of the transport processes that may occur in these cytosolic channels is concerned. Before we further discuss implications of this insight, we have to turn to the question: how reliable is our knowledge of plasmodesmal pore structure?

3. Picturing holes that are too small to see

Technological advances are often the basis for the transformation of scientific fields, and so it was with the development of electron microscopes. The first transmission electron microscopes (TEM) were built in the 1930s, and commercial instruments with resolutions below 1 nm became available in the middle of the century (Bozzola and Russell, 1999). However, it took another few decades until a true breakthrough in the life sciences could be achieved. This was mainly due to the necessary development of ancillary equipment like the ultramicrotome, and of fixatives that preserved, more or less, the ultrastructure of biological specimens. A patent for the industrial production of glutaraldehyde in the late 1950s provided a new, very potent disinfectant (Bedino, 2003) that soon turned out to be a superior preservative for the chemical fixation of biological samples. This was the final puzzle piece to establish electron microscopy as a fundamental technology in the life sciences. Starting in the 1960s, the description of the ultrastructure of cells and their organelles transformed our understanding of the functioning of living organisms. The following decades brought a variety of new technologies such as scanning electron microscopy (SEM), cryo-electron microscopy, electron tomography, and environmental electron microscopy. Atomic resolution is now routinely achieved in the material sciences and engineering, but also in certain fields of the life sciences. Unfortunately, similar degrees of improvement could not be accomplished in various types of cells and their components including plasmodesmata.

In a TEM, electrons are emitted from an electron gun and travel at roughly half the speed of light through the vacuum in the column of the microscope before they pass through the specimen and finally hit the detector (for a comprehensive treatment of the technology, see Reimer and Kohl, 2008). The incoming electrons may be deflected by the atoms in the specimen, causing dark spots on the screen – a phenomenon called contrast. Specimens must be thin enough to permit transmission by electrons, and have to be stable under the high vacuum inside the TEM. Therefore slices 50–100 nm thick are sectioned from biological samples with ultramicrotomes equipped with glass or diamond knifes, or, more recently, with focused ion beams. To prevent movements within samples in the process of ultrathin sectioning, the specimens need to be solid. This is achieved by replacing the water in the object by a resin that can be hardened to a plastic. Since most (epoxy) resins are insoluble in water, the sample is dehydrated in increments with a solvent that is compatible with the resin (usually methanol, ethanol, or acetone). To reduce artifact formation during water removal, prior fixation of the sample is necessary. The most frequently applied technique is chemical fixation. Chemical fixatives such as glutaraldehyde create a three-dimensional polymer that integrates and cross-links cellular components. After fixation, the replacement of water with solvent, and the replacement of solvent with resin, the resin is cured, and the specimen can be sectioned. An alternative approach is cryofixation and freeze substitution (not to be confused with cryo-electron microscopy discussed below). The sample is prefixed by rapid freezing before the water is replaced by liquid acetone containing chemical fixative at −80 °C. The tissue then is infiltrated by resin at normal temperature.

Numerous variations of the above protocols have been developed for different cells and tissues, but a fundamental problem remains: signal-to-noise ratios in TEM imaging depend critically on the mass of the atoms to be observed. Large atoms with numerous protons in their nuclei and correspondingly large electron shells interact efficiently with the incident electrons. For this reason, atomic resolution is routinely produced with specimens consisting of heavy atoms. In contrast, organic matter consists mostly of carbon, hydrogen, and oxygen, light atoms that interact weakly with incident electrons, which results in poor signal-to-noise ratios. Therefore, stains containing heavy metals such as uranyl acetate, potassium permanganate, lead citrate, or osmium tetroxide are applied to provide contrast. However, it is difficult to predict which cellular and molecular structures will be stained by a certain agent, and there always is a possibility that important features remain hidden because of lacking affinity of the stains applied. In any case, what we see in the TEM is not the native structure but the contrasting agent. This limits the achievable resolution, of course.

To clarify the consequences of this often underestimated problem, we return to the plasmodesmata that supposedly mediate the polymer trap mechanism. These pores let sucrose pass but exclude heavier oligosaccharides. For our argument's sake, we set the strongly simplifying premise that pore geometry alone controls pore permeability (for a more realistic approach, see Comtet et al., 2017). Since the hydrodynamic radius of sucrose molecules is about 0.47 nm (Wang and Fisher, 1994), the size-limiting cytosolic sleeve through which sucrose but no larger oligosaccharides move is expected to have a width of at least 1 nm, but not much more. Assuming 6 nm thickness for both the plasma and ER membrane, we arrive at the crude model shown as Fig. 5A. If we prepared a cross-section of this structure (Fig. 5B) for TEM observation, what we actually would see would be the contrast generated by the stain that bound or precipitated close to the biological structures due to some kind of affinity. We usually do not know where a given staining substance attaches and how many layers of the substance develop, as this depends, in addition to the nature of the stained object, on staining period, section thickness, resin hardness, location and environment of the structure within the sample, and other factors. For instance, the standard stain uranyl acetate produces uranyl ions (UO_2^{2+}) that bind to negatively charged biomolecules. UO_2^{2+} and similar staining ions have sizes of around 0.5 nm (Oda and Aoshima, 2002). Thus, it will take only a single layer of these ions on the inner walls of a 1 nm pore to occlude the pore. Cross-sections of our crude model will look differently depending on where the stain binds; examples given in Fig. 5 are preferential precipitation on cell wall material (Fig. 5C), on sectional surfaces of membranes (Fig. 5D), and on unobstructed membrane surfaces (Fig. 5E). Note that the cytosolic sleeve, the pathway for symplasmic transport, is not identified in Fig. 5A, whereas it is positively stained in Fig. 5 but negatively stained in Fig. 5E.

Despite their over-simplifying character, the sketches in Fig. 5 provide an impression of the ambiguities involved in the interpretation of TEM micrographs, which necessarily depends on assumptions about the mechanisms and results of the staining procedure. To demonstrate the relevance of this fact, we reproduced five previously published TEM micrographs of plasmodesma cross-sections at the same scale as our crude model (Fig. 5A) in Fig. 5F. We invite our readers to identify plasma membrane and cytosolic sleeve in these images. Subsequent comparison with the interpretations favored by the authors in the source papers

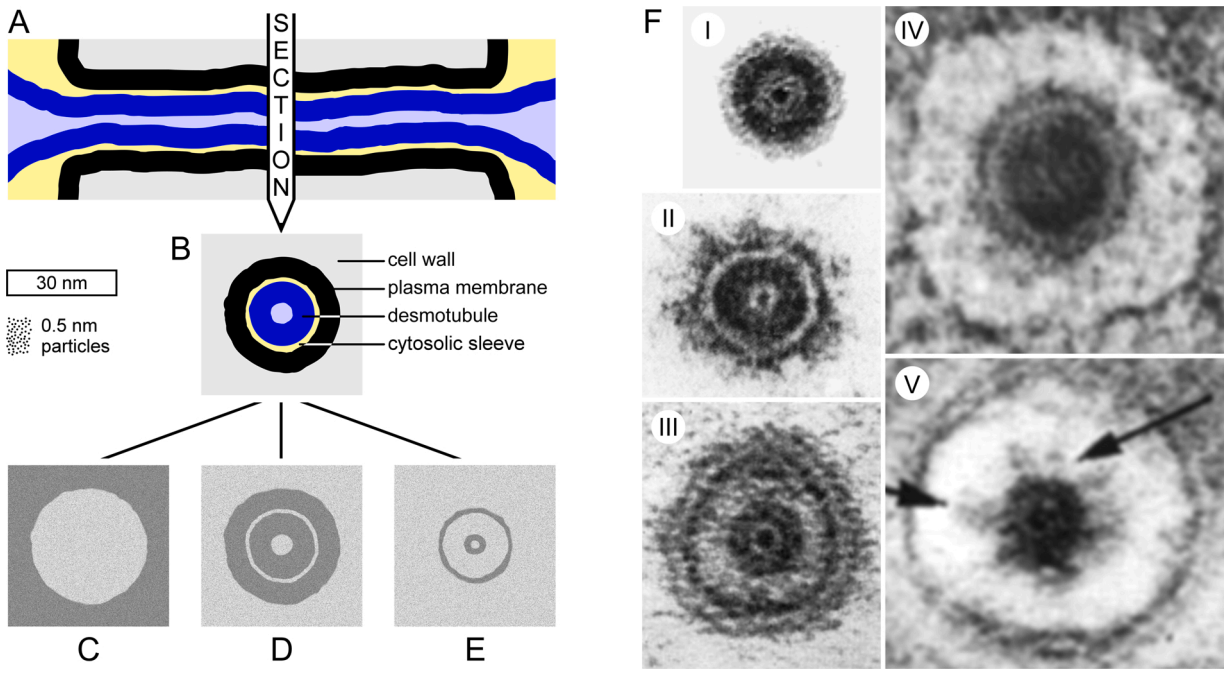

Fig. 5. Simplified model of a cylindrical plasmodesma (A-E) and reproductions of previously published TEM micrographs of plasmodesma cross-sections (F), all shown at the same scale (scale bar at the center left). The simplified model is shown in side view (A) and cross-section (B); the cell wall pore has an inner diameter of 30 nm, plasma membrane (black) and the ER membrane (blue) are 6 nm thick, and the cytosolic sleeve (yellow) is 1 to 1.5 nm wide, presumably allowing passage of sucrose (hydrodynamic radius 0.47 nm) but not of larger molecules. Contrasting stain used for transmission electron microscopy is assumed to consist of particles of 0.5 nm diameter (indicated under the scale bar for size comparison). Micrographs of cross-sections will appear differently depending on which biological components the staining substance binds. Examples show preferential binding to cell wall material (C), to sectional faces of membranes (D), and to accessible surfaces of membranes (E). In (E), the surfaces to which the stain binds are oriented perpendicular to the plane of sectioning, and the cytosolic sleeve is occluded by the stain. The sleeve is not identified in (C), while it appears light in (D) but dark in (E). TEM micrographs (F) appear at the same scale as the model, and show plasmodesmata from *Saccharum* sp. (I; Robinson-Beers and Evert, 1991; Fig. 8, p. 311), *Azolla pinnata* (II; Overall et al., 1982; Fig. 14, p. 140), *Salix* sp. (III; Robards 1968; Fig. 1, p. 784), *Persea americana* (IV; Botha and Cross, 1999; Fig. 2J, p. 33), and *Avena sativa* (V; Burgess, 1971; Fig. 9, p. 89). Reproduced with permission.

listed in the figure legend (Fig. 5) might turn out surprising in some cases.

Another interesting example is found in the now classical paper by Ding et al. (1992). When added to a fixative, tannic acid modulates the outcome of subsequent staining procedures (Afzelius, 1992) and causes, for example, a negative staining of microtubules (Fujiwara and Link, 1982). The same had been widely assumed to hold for structures within plasmodesmata, a view debated by Ding et al. (1992) who argued that tannic acid caused plasmodesma structures to appear positively rather than negatively stained. In essence, the question is: do the dark or the light zones in the images represent open spaces in which material can move from cell to cell (compare Fig. 5D and E)? The interpretation by Ding and colleagues (Fig. 6), according to which the lumen of the cytosolic sleeve is unstained, became the preferred model presented in textbooks and review articles over the past 25 years. However, the micrograph reproduced here as Fig. 6A is from an importing leaf tissue of *Nicotiana tabacum* (Ding et al., 1992), and the cells of these tissues readily exchange proteins of up to 50 kD by non-targeted transport (Oparka et al., 1999). One of them, the intermediately sized GFP (27 kD), has an experimentally determined hydrodynamic radius of 2.82 nm (Terry et al., 1995). Due to diffusive hindrance (Fig. 4), a cylindrical pore would have to measure about 14 nm across to allow GFP diffusion at only 10 % of the diffusivity in bulk solution. But worse than that; the hydrodynamic radius of GFP actually is larger than the estimated diameter of the 'presumed transport channels' (2.5 nm; Ding et al., 1992, Table 1). A circle of 2.8 nm radius plotted next to the micrograph and the derived models visualizes the dilemma: there is no cavity anywhere in the plasmodesma that would be even remotely wide enough to accommodate GFP, let alone any larger molecules (Fig. 6). We emphasize that this is not a singular case. As mentioned in the Introduction, Nicolas et al. (2017) recently reported symplasmic GFP movement between cells that were connected only by plasmodesmata that on electron micrographs lacked cytosolic sleeves altogether. It seems difficult to avoid the obvious conclusion: at least in some cases, the internal plasmodesmal structure that we see in the TEM cannot possibly represent the pathways responsible for the symplasmic transport phenomena we observe in live tissues.

One might hope for an improvement of this situation through techniques that have enabled the visualization of individual protein molecules and viruses at almost atomic resolution. Objects of such small sizes can be imaged without major preparation, but like with all organic samples, the signal-to-noise ratios are poor. However, because noise is random while the structure of the particle is not, the computational combination of multiple individual pictures can improve image quality significantly. This 'single particle analysis' has been automated, leading to a large increase of protein structures determined by cryo-TEM (over 2000 in 2019 alone) and challenging Xray crystallography as the primary tool in structural biology (Callaway, 2020). Unfortunately, larger cellular structures such as desmotubules do not generally exhibit perfectly repetitive structures, so that the methodology cannot simply be transferred. Moreover, sample preparation for cryo-TEM requires vitrification, freezing that is quick enough – 10^4 °K s^{-1} or faster – to prevent water crystal formation in the sample (Moor, 1987). In general, dense cytoplasm behaves like a cryoprotectant. Consequently, meristematic tissues lend themselves to fixation by vitrification and cryo-TEM studies, whereas mature plant cells with fully developed vacuoles do not (Moor, 1987). We conclude that while cryo-TEM has facilitated numerous insightful studies, the requirement for vitrification and the poor signal-to-noise ratios limit its usefulness. Its application to plasmodesmata in functionally mature cells therefore remains difficult at this time. In the words of Roberts (2005, p. 8), 'we may again have reached an impasse where advances in plasmodesmal structural research are

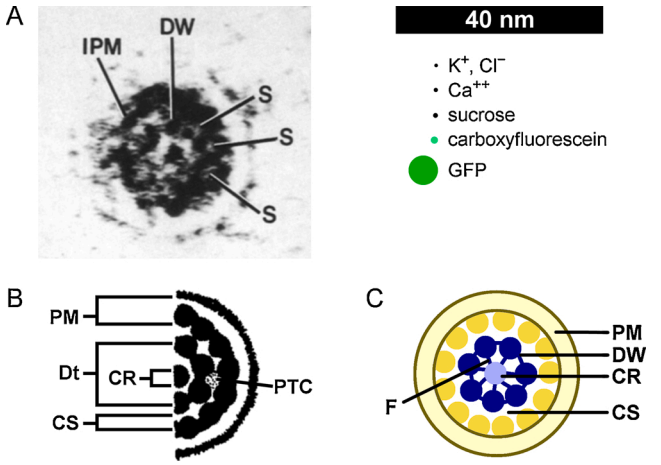

Fig. 6. Imaging and interpretation of plasmodesma structure in the classical paper by Ding et al. (1992). The graphs show an electron micrograph of a cross-section of a plasmodesma in a tobacco leaf (A; Fig. 6a, p. 35 in the original paper), its interpretation (B; originally Fig. 7b, p. 35, labeling redrawn), and a derived, generalized model (C; redrawn from Fig. 8c, p. 39 in the original paper. Reproduced with permission). The scale bar (top right) applies to all graphs. For comparison, sizes of some fully hydrated inorganic ions (Israelachvili, 2011, p. 79) and the hydrodynamic (Stokes) sizes of sucrose and the fluorescent tracer carboxyfluorescein (Wang and Fisher, 1994) as well as that of GFP (Terry et al., 1995) are indicated at the same scale. The tissue in which plasmodesmata as the one shown (A) are found is known to permit the non-targeted symplasmic transport of GFP and even larger proteins, which appear much too large to fit into the supposed open transport pathways marked S in (A), PTC in (B), and CS in (C). Labeling in the original: CR, central rod; CS, cytoplasmic sleeve; Dt, desmotubule; DW, desmotubule wall; F, filamentous structure; IPM, inner leaflet of the plasma membrane; PM, plasma membrane; PTC, presumed transport channel; S, spaces between particles of the desmotubule wall and the inner leaflet of the plasma membrane.

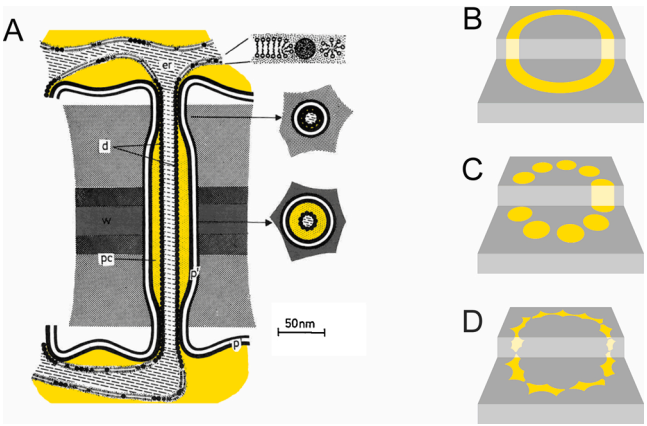

Fig. 7. Structural models of the cytosolic sleeve in plasmodesmata. (A) Model of a simple plasmodesma with desmotubule viewed in longitudinal and two transverse sections (from Robards, 1976; Fig. 2.7, p. 44. Color added to mark the cytoplasm). A wide cytosolic sleeve is present in the center of the structure, but not in the neck regions in which the cell wall pore is constricted (reproduced with permission). Later models of plasmodesmata reconstructed the sleeve as an annular channel (B), a radially arranged set of individual tubes (C), or a somewhat irregular network of spaces intersected by linkers between desmotubule and plasma membrane (D). See text for details.

concerned. Despite many comprehensive microscopical studies that have elucidated the general structures of plasmodesmata, the finer details may not be obtainable until future breakthroughs in imaging are made.'

4. Size and plasmodesma research: some of our blind spots

The electron microscopy methodologies discussed above have been utilized in various ways to design the plasmodesma models found in the current literature. When evaluating these models, we need to keep in mind that all of them are based on electron micrographs produced from samples subjected to heavy metal staining, with all of the limitations and potential problems discussed above.

4.1. Standard models imply electrokinetic effects

The first high-resolution reconstructions of the structure of simple plasmodesmata based on TEM micrographs by López-Sáez et al. (1966) and Robards (1968) already exhibited the essential features of current models. Robards (1976) compared a number of models which agreed in most structural characters. The plasmodesma was depicted as a cell wall pore of 30–60 nm diameter lined by the continuous plasma membrane and containing a desmotubule (Fig. 7a). The cytosolic sleeve, the narrow space between plasma membrane and desmotubule, was drawn 10–12 nm wide in most models, although the tabulated data suggested only half of that width in most cases (Robards, 1976, p. 46). The cell wall pore itself showed constricted neck regions at its openings to the cell lumina. In these neck regions the cytosolic sleeve was absent, and material exchange between cells seemed possible only through the ER. As evidence for cell-to-cell transport in the cytosol became available, later models (such as Fig. 6) focused on the role of the sleeve in the translocation of cytosolic components such as dissolved sugars. In the simplest case, the cytosolic sleeve could be envisioned as an annular channel (Fig. 7b; compare López-Sáez et al., 1966). Later authors suggested the sleeve to consist of circularly arranged, individual tubes (Fig. 7c; Comtet et al., 2017) or as irregular spaces between protein linkers that connected desmotubule and plasma membrane (Fig. 7d; Ding et al., 1992). If the widest diameter of the cell wall pore is in the range of 50 nm or below as suggested by the micrographs on which the models are based, the width of the cytosolic sleeve cannot be more than a few nm in any of these models. Thus, if we apply the IUPAC pore classification discussed above, cytosolic sleeves will qualify as narrow mesopores or even as micropores in any case. Consequently, the function of cytosolic sleeves cannot be analyzed as if they were macropores. As an example for the implications of this fact, let us consider electrical effects.

The inner leaflet of the eukaryotic plasma membrane is negatively charged due to the large proportion among its phospholipids of phosphatidylserine (Bigay and Antonny, 2012; Jackson et al., 2016) and in plants also of phosphatidylinositol (Simon et al., 2016). Consequently, electrical double-layer theory applies to the inner surface of the plasma membrane (McLaughlin, 1989), which in plasmodesmata is the structural equivalent of the wall surface in artificial nanochannels. Published data allow the estimation of charge densities of plant plasma membranes to be around $-0.03\ C\ m^{-2}$ (Kinraide and Wang, 2010). This value is derived from measurements that apparently reflect the character of the outer membrane surface, not the inner one which is more strongly charged. Therefore the magnitude of the charge density on the inner membrane surface in the living cell could be larger. It is worth emphasizing that the plasma membrane in plasmodesmata, although apparently characterized by a specific lipid composition, seems to have the same proportion of negatively charged phospholipids as the plant plasma membrane in general (see Supplemental Fig. 6 of Grison et al., 2015). Moreover, the recent model of an MCTP (Multiple C2 and Transmembrane domain-containing Protein)-mediated linkage between desmotubule and plasma membrane postulates an essential role for negative charges on the inner surface of the plasma membrane in tethering this membrane to the desmotubule (Brault et al., 2019). The assumption that the inner surface of the 'wall' of the plasmodesmal channel is negatively charged therefore is plausible. The effects of the negative charge of the plasmodesmal 'wall' will be especially pronounced if the center of the pore – which is farthest away from the

charged 'wall' – is occupied by a desmotubule and thus not available for the movement of particles in the cytosol. Therefore, based on established knowledge about artificial meso- and micropores (in the IUPAC definition of the terms) and on current structural models of plasmodesmata, it seems that the sleeves available for cytosolic transport in 'standard' plasmodesmata (Fig. 7) should be permselective, allowing entry of cationic solutes at significantly higher rates than that of anionic ones.

Permselective channels give rise to surprising phenomena. For example, mechanical interactions between the counter-ions and the other fluid components in channels of these dimensions can lead to electroosmotic flow (Burgreen and Nakache, 1964; Rice and Whitehead, 1965; Sparreboom et al., 2009; Haywood et al., 2015). If the counter-ions move along a permselective channel driven by an applied electrical field, they drag adjacent fluid layers in the same direction. Conversely, when the solution flows advectively through these channels, e.g. driven by a hydrostatic pressure gradient, electrical streaming currents are induced because counter-ions, which easily enter the channel, dominate in the moving fluid over co-ions, which are excluded from the channel (Fig. 8). The resulting streaming potential drives an electroosmotic backflow against the direction of the pressure-driven flow. This decreases the net flow rate and increases the apparent viscosity of the moving fluid, which is known as the electroviscous effect (Bandopadhyay et al., 2014).

Intriguingly, electrokinetic phenomena play an insignificant role in current debates about plasmodesma function, which appear dominated by the idea that 'hydrodynamic radius alone governs the mobility of molecules through plasmodesmata' (Terry and Robards, 1987). But if basic knowledge about the composition of cellular membranes and the cytosol is valid for plasmodesmata, and if the physical principles governing the functions of artificial nanometer-sized channels are applicable also to biological systems, elektrokinetic effects must play significant roles in the latter – which presents a conundrum. Consider the fluorescent tracers we frequently utilize to monitor symplasmic connectivity (Oparka and Boevink, 2005; Knoblauch et al., 2015). Particularly useful tracers such as carboxyfluorescein remain within cells once they have entered the cytoplasm, due to their electrical charges that render them membrane-impermeant. At pH 7.0–7.5, typical of the plant cell cytosol, carboxyfluorescein molecules are anionic, most of them trivalent (Weinstein et al., 1986). These anions certainly have no problem passing through macropores (in the IUPAC definition) such as sieve pores, which makes them a powerful tool for monitoring symplasmic mass flow in sieve tubes (Grignon et al., 1989). But they definitely should be excluded from meso- and micropores with negatively charged 'walls'. Nonetheless, carboxyfluorescein moves through plasmodesmata in live tissues at surprisingly high rates (Rutschow et al., 2011).

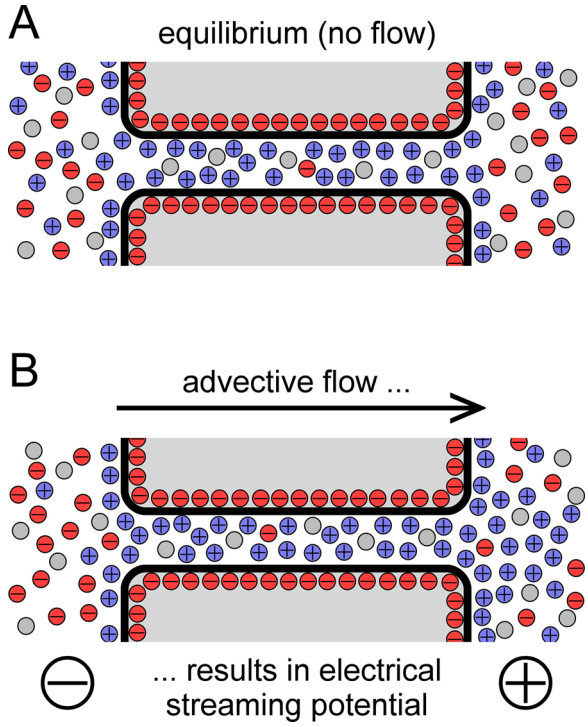

Fig. 8. Electrokinetic effects observed in nanofluidics systems. (A) Permselective channel with electrically charged, in this case anionic walls. The channel radius is similar to the electrical double layer thickness, so that counter-ions and uncharged particles readily enter the channel while co-ions are mostly excluded. (B) Advective flow driven by a pressure gradient causes charge separation because of the differential access of ions into the channel. This generates a so-called streaming potential that drives counter-ions against the advective flow, creating an electroosmotic backflow. As a result, the net flow through the channel will be less than expected based on pore size, fluid viscosity, and the driving force for advective flow (electroviscous effect).

4.2. *Structural dynamics through thermal motion*

In the macroscopic realm, Brownian or thermal motion is perceptible as heat, but does not move objects. Therefore it can be ignored when the movements of animals, tidal waves, or planets are analyzed. This is not so when we evaluate the behavior of objects of microscopic or molecular dimensions. Thermal motion has important implications for our interpretation of images produced with the electron microscope as well as for possible regulatory mechanisms of plasmodesma function.

In 1978, Richard P.C. Johnson published a study on 'The microscopy of P-protein filaments in freeze-etched sieve pores', in which he evaluated the thermal motion of particles during the short period needed for rapid fixation of specimens for electron microscopy. The scientific background was the debate about the open or closed state of sieve pores, and the question whether bulk flow in sieve tubes, which requires open sieve pores, was at all possible (for review, see Knoblauch and Peters, 2017). Filaments of so-called P-proteins had frequently been detected in sieve pores, which they seemed to occlude. Johnson's conclusion is worth quoting:

> 'The entire width of most of the sieve pores seen contained filaments separated by less than 100 nm. Their arrangement indicates too high a resistance to flow for pressure flow alone to drive translocation at known rates … However, calculations are presented to show that during the time taken to fix the pores, by fast freezing or chemically, the filaments in them could rearrange and move further by Brownian and other motion than the distances between filaments which we need to measure. These calculations show that it is not possible, by microscopy alone, to answer the outstanding question "How are filaments arranged in translocating sieve pores?" with enough certainty to tell us whether pressure flow is adequate to explain translocation where filaments are present. The calculations are relevant also to microscopy of other cell structures which may move.' (Johnson, 1978, p. 191).

Notably, the protein filaments whose movements Johnson was interested in measured 16 nm in diameter and were located in pores about 0.75 μm wide (Johnson, 1978, p. 202). 'Typical' plasmodesmata as discussed above (compare Figs. 5–7) and the structures within them are an order of magnitude smaller. Thermal motion therefore should have an even more significant impact in plasmodesmata than in the sieve pores Johnson studied. Unfortunately, Johnson's work is all but forgotten; according to the Web-of-Science database, Johnson (1978) was cited only four times in the last 30 years. We feel, though, that his work provides insights that may be helpful in reconstructing plasmodesma structure, for example concerning the reality of measurements of cytosolic sleeve width taken from electron micrographs.

Thermal motion of structural components of plasmodesmata and

other channels is not only a nuisance to electron microscopists like Johnson, it may actually be part of the transport and gating mechanisms operating in these structures. As an example, consider a plasmodesma of circular cross-section with an inner diameter, measured between the inner surfaces of the plasma membrane, of *D*, and a desmotubule of outer diameter 0.5 *D* (Fig. 9). As long as the desmotubule is located in the center of the plasmodesma, the cytosolic sleeve will be an annular space 0.25 *D* wide. But if, due to random thermal motion, the desmotubule swings to one side until it touches the plasma membrane, the sleeve turns into a space through which spheres of up to 0.5 *D* diameter could pass. It follows from these trivial geometric considerations that when we think about the possible transport of spherical, electrically neutral particles of say 0.4 *D* diameter, the plasmodesma exists in either of two states: closed, when the desmotubule is located more or less in the channel's center, and open, when it is located in the periphery. In contrast, the plasmodesma is open at all times for uncharged particles with 0.1 *D* diameter. Importantly, the presence of 0.4 *D* particles in the cytosolic sleeve will lock the plasmodesma in the open state, because the desmotubule could not swing back into a central position. Therefore the plasmodesma would be cargo-gated; it will remain open for 0.4 *D* particles because it already is transporting them. It seems plausible that the frequency of the cargo-gated open state should depend on the rate at which 0.4 *D* particles enter the sleeve, in other words, on the concentration of the particles on the source side of the plasmodesma.

In support of our hypothesizing about cargo-gating, or a cargo-induced transport capacity that requires thermal motion of the desmotubule, we notice, first, that recent ultrastructural studies seemed to show the desmotubule as a flexible rod that may be attached to the plasma membrane at certain points along its length while apparently free floating in the center of the pore between those attachment points (Nicolas et al., 2017). Subsequent analyses focused on the identity of the molecules potentially involved in mediating the apparent plasma membrane/ER attachments (Brault et al., 2019; Petit et al., 2020). However, the most important conclusion in our present context is that

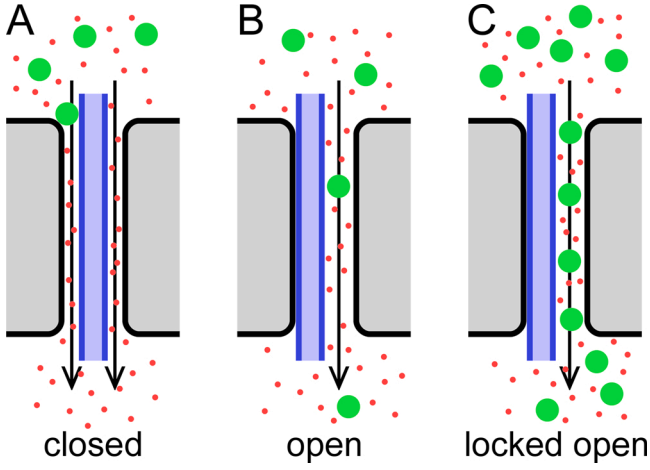

Fig. 9. Simple model of a plasmodesma in a cell wall (gray) with a desmotubule (blue), showing the hypothetical cargo-gating mechanism. Cartoons are drawn to scale; the outer diameter of the desmotubule (0.5 *D*) is half the inner diameter of the pore (*D*). Two classes of particles are shown, large (green; diameter 0.4 *D*) and small (red; diameter 0.1 *D*). The desmotubule changes its position in the pore continuously due to thermal motion. The small particles can move through the sleeve between the wall of the pore (plasma membrane, thick black line) and the desmotubule regardless of the position of the latter. In contrast, for the large particles the plasmodesma is effectively closed when the desmotubule is in a central position (A) whereas it is open with the desmotubule in the periphery (B). If the concentration of large particles is sufficiently high, cargo-gating may occur: the permanent presence of large particles in the sleeve locks the plasmodesma in the open state (C) by sterically preventing the movement of the desmotubule from its peripheral position.

the conventional picture of the desmotubule fixed in the center of the plasmodesma (e.g., Figs. 6C, 7 A) might have to be replaced by more dynamic models allowing for thermal movement of the desmotubule within the pore. Second, Ross-Elliott and colleagues (2017) analyzed symplasmic phloem unloading in the root growth zone of *Arabidopsis* by fluorescence recovery after photobleaching (FRAP). Green fluorescent protein (27 kDa) and larger fluorescent tracers ranging up to 112 kDa did not move from sieve tubes to surrounding cells at constant rates, but in distinct pulses. The authors referred to this phenomenon as 'batch unloading'. In contrast, smaller molecules such as carboxyfluorescein (0.38 kDa) and esculin (0.34 kDa) exited the sieve tubes at constant rates over prolonged periods. This pattern is strikingly similar to what our cargo-gating model suggests (Fig. 9). It remains to be seen whether a biological significance for such a surprisingly simply mechanism can be established experimentally.

4.3. Plasmodesma clusters

Last but not least, we emphasize that despite the urgent need to better understand the physical nature of transport processes that occur in a single plasmodesma, the structural context has to be considered to obtain a full picture of the plasmodesma's biological function. For instance, consider two compartments separated by an impermeable wall with a pore of cross-sectional area *A*. Given a defined concentration gradient of a diffusible substance between the compartments, the diffusive net transport through the pore will be far greater than it would be across an area of size *A* in the plane between the compartments if there were no wall between them at all. Ultimately this is because the concentration gradients around the openings of pores are dome-shaped and thus tend to dissipate faster. Consequently, diffusion through a perforated wall will be faster than predicted from the sum of the cross-sectional pore areas. The effect becomes less pronounced with increasing pore densities, because the diffusion shells at the openings of individual pores exert increasing influence on each other at higher densities. The physical basis of these phenomena has been quantitatively analyzed over a century ago by Brown and Escombe (1900); two figures from this classical work are reproduced in our Fig. 10 (for more recent visualizations, see e.g. Roth-Nebelsick, 2007).

Modified and extended versions of the theory of Brown and Escombe (1900) have been utilized widely in studies of evaporation through stomata (Seybold, 1929; Ting and Loomis, 1963, 1965; Zwienicki et al., 2016), but we are not aware of an application of the theory to clusters of plasmodesmata in the newer literature. This seems remarkable, since Brown and Escombe (1900) stressed the value of their formalism for understanding the role of the cytoplasmic bridges not yet named plasmodesmata in the diffusive transport of materials between cells. In fact, Strasburger (1901, pp. 539-540) highlighted their work for the same reason. With reference to pairs of pits separated by pit membranes with multiple plasmodesmata (Fig. 1J), Brown and Escombe (1900, p. 281) explained: 'the flow of the diffusing substance … may go on almost as rapidly through the multi-perforate septum as if no closing membrane were present'. We think that integrating appropriately modernized versions of the theory into current quantitative models can only help our understanding of the biological significance of plasmodesmal transport.

5. Concluding remark

Historically, cytoplasmic cell-to-cell bridges of all sizes were called plasmodesmata. With the advent of the electron microscope and its application to plant cells, the definition changed. This change remained implicit, but plant biologists today undoubtedly understand plasmodesmata to be nanometer-sized pores. The dominance of various electron microscopy techniques as tools for elucidating the structure of such 'nanopores' creates its own problems. By their very nature, electron micrographs mask the dynamics that may be functionally essential in the structures under study. But more than this: the micrographs do not

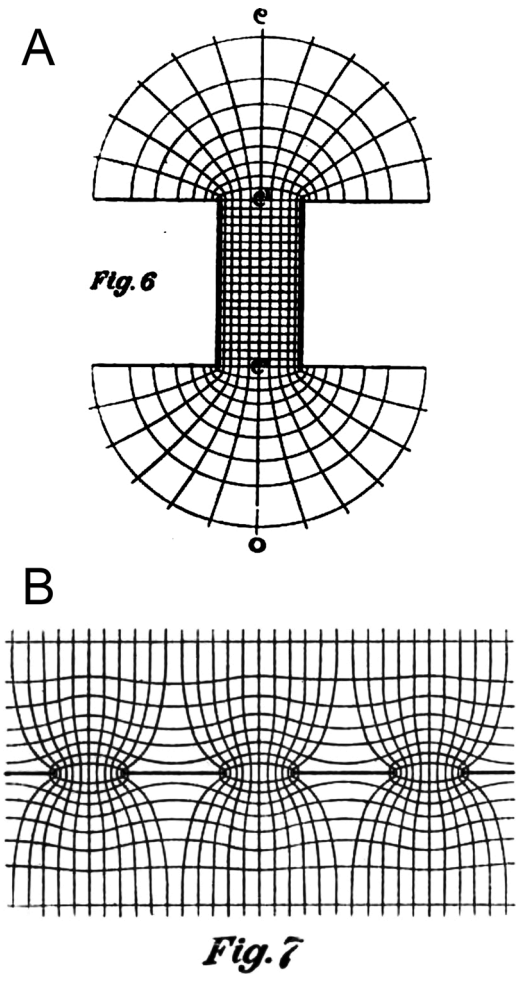

Fig. 10. Diffusion through pores as analyzed by Brown and Escombe (1900). (A) Diffusion through a cylindrical pore in a wall or membrane, from maximum concentration of the diffusing substance ρ (top) to 0 (bottom). Lines running parallel with the pore's axis are trajectories of net diffusion, lines perpendicular to the pore's axis represent planes of equal concentration. Concentration gradients on both sides of the pore are steep as the diffusing particles can approach (top) or leave the pore (bottom) in many directions, as indicated by the spreading of the trajectories. Given identical concentration gradients (ρ to 0), the net flow rate across the cross-sectional area of the pore is significantly higher than across the identical area in the absence of the wall. (B) Three pores in a wall (shown here as a thick horizontal line). Concentration gradients are less steep compared to A, because the trajectories corresponding to different pores interfere with each other, reducing their spread. This situation approaches diffusion in the absence of any wall.

represent reality in the same sense in which a photograph of a flowering *Arabidopsis* in its natural habitat does. Electron micrographs present cellular structures in highly artificial states, following significant modifications of their chemical and physical properties as well as the addition of materials with the explicit purpose of modifying the appearance of the specimens. Therefore these images require careful interpretation. This is not a novel insight, of course, and it has been suggested before that structural features of plasmodesmata 'not visible on standard transmission electron micrographs may have strong influence on permeability' (Liesche et al., 2019, p. 1768). But if these important structural features are obscured on electron micrographs for currently unavoidable methodological reasons, we maybe should let Richard Johnson remind us that there is 'little point in continuing to argue about a crucial observation which cannot, in fact, be made' (Johnson, 1978, p. 204). For now, we rather may accept the fact that the plasmodesma models we design based on available ultrastructural data are speculative at best. Whether it helps that we keep reproducing these models in the textbooks we ask our students to read is an interesting question. We feel that smart, physically inspired guesses founded on our growing understanding of artificial nanofluidics systems actually may lead to more realistic ideas on how plasmodesmata accomplish what we think they do in living plants.

Declaration of Competing Interests

There are no competing interests to declare.

Acknowledgments

We thank Jan Knoblauch for providing the fluorescence micrograph in our Fig. 1I. This work was supported by grants NSF 1656769 and NSF 1940827 to M.K.

References

Abounit, S., Zurzolo, C., 2012. Wiring through tunneling nanotubes – from electrical signals to organelle transfer. J. Cell. Sci. 125, 1089–1098.
Afzelius, B.A., 1992. Section staining for electron microscopy using tannic acid as a mordant: a simple method for visualization of glycogen and collagen. Microsc. Res. Tech. 21, 65–72.
Baker, J.R., 1952. The cell-theory: a restatement, history and critique. Part III. The cell as a morphological unit. Quart. J. Microscop. Sci. 93, 157–190.
Bandopadhyay, A., Hossain, S.S., Chakraborty, S., 2014. Ionic size dependent electroviscous effects in ion-selective nanopores. Langmuir 30, 7251–7258.
Barton, D.A., Cole, L., Collings, D.A., Liu, D.Y.T., Smith, P.M.C., Day, D.A., Overall, R.L., 2011. Cell-to-cell transport via the lumen of the endoplasmic reticulum. Plant J. 66, 806–817.
Bedino, J.H., 2003. Embalming chemistry: glutaraldehyde versus formaldehyde. Champion Expanding Encyclopedia of Mortuary Practices. Article Number 649.
Beebe, D.J., Mensing, G.A., Walker, G.M., 2002. Physics and applications of microfluidics in biology. Annu. Rev. Biomed. Eng. 4, 261–286.
Behnke, H.-D., 1990. Cycads and gnetophytes. In: Behnke, H.-D., Sjolund, R.D. (Eds.), Sieve Elements. Springer, Berlin, pp. 89–101.
Bigay, J., Antonny, B., 2012. Curvature, lipid packing, and electrostatics of membrane organelles: defining cellular territories in determining specificity. Dev. Cell 23, 886–895.
Billings, S.M., 1971. Concepts of nerve fiber development, 1839–1930. J. Hist. Biol. 4, 275–305.
Bloemendal, S., Kück, U., 2013. Cell-to-cell communication in plants, animals, and fungi: a comparative review. Naturwissenschaften 100, 3–19.
Bocquet, L., Charlaix, E., 2010. Nanofluidics, from bulk to interfaces. Chem. Soc. Rev. 39, 1073–1095.
Bose, J.C., 1926. The Nervous Mechanism of Plants. Longmans, Green and Co., London.
Botha, C.E.J., Cross, R.H.M., 1999. Plasmodesmal imaging – towards understanding structure. In: van Bel, A.J.E., van Kesteren, W.J.P. (Eds.), Plasmodesmata. Springer, Berlin, pp. 27–36.
Bozzola, J.J., Russell, L.D., 1999. Electron Microscopy: Principles and Techniques for Biologists, 2nd ed. Jones and Bartlett, Sudbury MA, USA.
Brault, M.L., Petit, J.D., Immel, F., Nicolas, W.J., Glavier, M., Brocard, L., Gaston, A., Fouché, M., Hawkins, R.J., Crowet, J.-M., Grison, M.S., Germain, V., Rocher, M., Kraner, M., Alva, V., Claverol, S., Paterlini, A., Helariutta, Y., Deleu, M., Lind, L., Tilsner, J., Bayer, E.M., 2019. Multiple C2 domains and transmembrane region proteins (MCTPs) tether membranes at plasmodesmata. EMBO Rep. 20, e47182.
Brown, H.T., Escombe, F., 1900. Static diffusion of gases and liquids in relation to the assimilation of carbon and translocation in plants. Philos. Trans. R. Soc. B 193, 223–292.
Bruno, G., di Trani, N., Hood, R.L., Zabre, E., Filgueira, C.S., Canavese, G., Jain, P., Smith, Z., Demarchi, D., Hosali, S., Pimpinelli, A., Ferrari, M., Grattoni, A., 2018. Unexpected behaviors in molecular transport through size-controled nanochannels down to the ultra-nanoscale. Nat. Commun. 9, 1682.
Burch-Smith, T.M., Zambryski, P.C., 2012. Plasmodesmata paradigm shift: regulation from without versus within. Annu. Rev. Plant Biol. 63, 239–260.
Burgess, J., 1971. Observations on structure and differentiation in plasmodesmata. Protoplasma 73, 83–95.
Burgreen, D., Nakache, F.R., 1964. Electrokinetic flow in ultrafine capillary slits. J. Phys. Chem. 68, 1084–1091.
Callaway, E., 2020. The protein-imaging technique taking over structural biology. Nature 578, 201.
Carr, D.J., 1976. Historical perspectives on plasmodesmata. In: Gunning, B.E.S., Robards, A.W. (Eds.), Intercellular Communication in Plants: Studies on Plasmodesmata. Springer, Berlin, pp. 291–295.
Cervera, J., Schiedt, B., Neumann, R., Mafé, S., Ramírez, P., 2006. Ionic conduction, rectification, and selectivity in single conical nanopores. J. Chem. Phys. 124, 104706.

Cervera, J., Pietak, A., Levin, M., Mafe, S., 2018. Bioelectrical coupling in multicellular domains regulated by gap junctions: a conceptual approach. Bioelectrochemistry 123, 45–61.
Choi, W.-G., Hilleary, R., Swanson, S.J., Kim, S.-H., Gilroy, S., 2016. Rapid, long-distance electrical and calcium signaling in plants. Annu. Rev. Plant Biol. 67, 287–307.
Comtet, J., Turgeon, R., Stroock, A.D., 2017. Phloem loading through plasmodesmata: a biophysical analysis. Plant Physiol. 175, 904–915.
Cook, M.E., Graham, L.E., 1999. Evolution of plasmodesmata. In: van Bel, A.J.E., van Kesteren, W.J.P. (Eds.), Plasmodesmata. Springer, Berlin, pp. 101–117.
Corry, B., Kuyucak, S., Chung, S.-H., 2000. Tests of continuum theories as models of ion channels. II. Poisson-Nernst-Planck theory versus Brownian dynamics. Biophys. J. 78, 2364–2381.
Crawford, K.M., Zambryski, P.C., 2001. Non-targeted and targeted protein movement through plasmodesmata in leaves in different developmental and physiological states. Plant Physiol. 125, 1802–1812.
Dechadilok, P., Deen, W.M., 2006. Hindrance factors for diffusion and convection in pores. Ind. Eng. Chem. Res. 45, 6953–6959.
Dhavale, T., Jedd, G., 2007. The fungal Woronin body. In: Howard, R.J., Gow, N.A.R. (Eds.), Biology of the Fungal Cell. The Mycota VIII, 2nd ed. Springer, Berlin, pp. 87–96.
Ding, B., Turgeon, R., Parthasarathy, M.V., 1992. Substructure of freeze-substituted plasmodesmata. Protoplasma 169, 28–41.
Ding, B., Itaya, A., Woo, Y.M., 1999. Plasmodesmata and cell-to-cell communication in plants. Intern. Rev. Cytol. 190, 251–316.
Ehlers, K., Kollmann, R., 2001. Primary and secondary plasmodesmata: structure, origin, and functioning. Protoplasma 216, 1–30.
Ehlers, K., van Bel, A.J.E., 2010. Dynamics of plasmodesmal connectivity in successive interfaces of the cambial zone. Planta 231, 371–385.
Eleftheriou, E.P., 1990. Monocotyledons. In: Behnke, H.-D., Sjolund, R.D. (Eds.), Sieve Elements. Springer, Berlin, pp. 139–159.
Esau, K., Charvat, I., 1978. On vessel member differentiation in the bean (*Phaseolus vulgaris* L.). Ann. Bot. 42, 665–677.
Esau, K., Thorsch, J., 1985. Sieve plate pores and plasmodesmata, the communication channels of the symplast: ultrastructural aspects and developmental relations. Am. J. Bot. 72, 1641–1653.
Evert, R.F., 1990. Dicotyledons. In: Behnke, H.-D., Sjolund, R.D. (Eds.), Sieve Elements. Springer, Berlin, pp. 103–137.
Evert, R.F., 2006. Esau's Plant Anatomy, 3rd ed. Wiley Interscience, Hoboken NJ.
Falkner, C., Akman, O.E., Bell, K., Jeffree, C., Oparka, K., 2008. Peeking into pit fields: a multiple twinning model of secondary plasmodesmata formation in tobacco. Plant Cell 20, 1504–1518.
Falkovich, G., 2018. Fluid Mechanics, 2nd ed. Cambridge University Press, Cambridge.
Fromm, J., Lautner, S., 2007. Electrical signals and their physiological significance in plants. Plant Cell Environ. 30, 249–257.
Fujiwara, K., Link, R.W., 1982. The use of tannic acid in microtubule research. In: Wilson, L. (Ed.), Methods in Cell Biology. Academic Press, New York, pp. 217–233.
Goldberg, G.S., Valiunas, V., Brink, P.R., 2004. Selective permeability of gap junction channels. Biochim. Biophys. Acta 1662, 96–101.
González-Méndez, L., Gradilla, A.-C., Guerrero, I., 2019. The cytoneme connection: direct long-distance signal transfer during development. Development 146, dev174607.
Grabski, S., de Feijter, A.W., Schindler, M., 1993. Endoplasmic reticulum forms a dynamic continuum for lipid diffusion between contiguous soybean root cells. Plant Cell 5, 25–38.
Grignon, N., Touraine, B., Durand, M., 1989. 6(5)carboxyfluorescein as a tracer of phloem sap translocation. Am. J. Bot. 76, 871–877.
Grison, M.S., Brocard, L., Fouillen, L., Nicolas, W., Wewer, V., Dörmann, P., Nacir, H., BenitezAlfonso, Y., Claverol, S., Germain, V., Boutté, Y., Mongrand, S., Bayer, E.M., 2015. Specific membrane lipid composition is important for plasmodesmata function in *Arabidopsis*. Plant Cell 27, 1228–1250.
Hancock, J.T., 2005. Cell Signalling, 2nd ed. Oxford University Press, Oxford.
Hanstein, J., 1864. Die Milchsaftgefässe und die verwandten Organe der Rinde. Wiegandt und Hempel, Berlin.
Hartig, T., 1837. Vergleichende Untersuchungen über die Organisation des Stammes der einheimischen Waldbäume. Jahresber. Fortschr. Forstwissensch. forstl. Naturk. 1, 125–168 (with Table I).
Haywood, D.G., Saha-Shah, A., Baker, L.A., Jacobson, S.C., 2015. Fundamental studies of nanofluidics: nanopores, nanochannels, and nanopipets. Anal. Chem. 87, 172–187.
Heinlein, M., 2015. Plant virus replication and movement. Virology 479–480, 657–671.
Held, H., 1906. Zur Histogenese der Nervenleitung. Anat. Anz. 29, 185–205 (Ergänzungsheft).
Hepler, P., 1982. Endoplasmic reticulum and the formation of the cell plate and plasmodesmata. Protoplasma 111, 121–133.
Hillhouse, W., 1883. Einige Beobachtungen über den intercellularen Zusammenhang von Protoplasten. Bot. Centralbl. 14 (89–94), 121–125 (with Table III).
Holt, J.K., Park, H.G., Wang, Y., Stadermann, M., Artyukhin, A.B., Grigoropoulos, C.P., Noy, A., Bakajin, O., 2006. Fast mass transport through sub-2-nanometer carbon nanotubes. Science 312, 1034–1037.
Hsu, J.-P., Chen, Y.C., Chen, Y.-M., Tseng, S., 2018. Influence of temperature and electroosmotic flow on the rectification behavior of conical nanochannels. J. Taiwan Inst. Chem. Eng. 93, 142–149.
Hsu, J.-P., Chu, Y.-Y., Lin, C.-Y., Tseng, S., 2019. Ion transport in a pH-regulated conical nanopore filled with a power-law fluid. J. Colloid Interface Sci. 537, 358–365.
Imlau, A., Truernit, E., Saur, N., 1999. Cell-to-cell and long-distance trafficking of the green fluorescent protein in the phloem and symplastic unloading of the protein into sink tissues. Plant Cell 11, 309–322.
Israelachvili, J.N., 2011. Intermolecular and Surface Forces, 3rd ed. Elsevier, Amsterdam.
Jackson, D., 2005. Transcription factor movement through plasmodesmata. In: Oparka, K.J. (Ed.), Plasmodesmata. Blackwell Publishing, Oxford, pp. 113–134.
Jackson, C.L., Walch, L., Verbavatz, J.-M., 2016. Lipids and their trafficking: an integral part of cellular organization. Dev. Cell 39, 139–153.
Jensen, K.H., Mullendore, D.L., Holbrook, N.M., Bohr, T., Knoblauch, M., Bruus, H., 2012. Modeling the hydrodynamics of sieve plates. Front. Plant Sci. 3, 151.
Johnson, R.P.C., 1978. The microscopy of P-protein filaments in freeze-etched sieve pores. Planta 143, 191–205.
Kandel, E.R., Schwartz, J.H., Jessell, T.M., Siegelbaum, S.A., Hudspeth, A.J., 2012. Principles of Neural Science, 5th ed. McGraw-Hill, New York.
Kay, R., Smith, J. (Eds.), 1989. The Molecular Basis of Positional Signaling. The Company of Biologists Ltd, Cambridge.
Kehr, J., Kragler, F., 2018. Long distance RNA movement. New Phytol. 218, 29–40.
Kienitz-Gerloff, F., 1891. Die Protoplasmaverbindungen zwischen benachbarten Gewebselementen in der Pflanze. Bot. Zeitg. 49, 65–74, 1–10, 17–26, 33–46, 49–60, (with Tables I, II).
Kinraide, T.B., Wang, P., 2010. The surface charge density of plant cell membranes (σ): an attempt to resolve conflicting values for intrinsic σ. J. Exp. Bot. 61, 2507–2518.
Knoblauch, M., Peters, W.S., 2004. Biomimetic actuators: where technology and cell biology merge. Cell. Mol. Life Sci. 61, 2497–2509.
Knoblauch, M., Peters, W.S., 2013. Long-distance translocation of photosynthates: a primer. Photosynth. Res. 117, 189–196.
Knoblauch, M., Peters, W.S., 2017. What actually is the Münch hypothesis? A short history of assimilate transport by mass flow. J. Integr. Plant Biol. 59, 292–310.
Knoblauch, M., Stubenrauch, M., van Bel, A.J.E., Peters, W.S., 2012. Forisome performance in artificial sieve tubes. Plant Cell Environ. 35, 1419–1427.
Knoblauch, M., Vendrell, M., de Leau, E., Paterlini, A., Knox, K., Ross-Elliot, T., Reinders, A., Brockman, S.A., Ward, J., Oparka, K., 2015. Multispectral phloem-mobile probes: properties and applications. Plant Physiol. 167, 1211–1220.
Köhler, P., Carr, D.J., 2006. Eduard Tangl (1848–1905) – discoverer of plasmodesmata. Huntia 12, 169–211.
Kollmann, R., Glockmann, C., 1999. Multimorphology and nomenclature of plasmodesmata in higher plants. In: van Bel, A.J.E., van Kesteren, W.J.P. (Eds.), Plasmodesmata. Springer, Berlin, pp. 149–172.
Kornberg, T.B., Roy, S., 2014a. Cytonemes as specialized signaling filopodia. Development 141, 729–736.
Kornberg, T.B., Roy, S., 2014b. Communicating by touch – neurons are not alone. Trends Cell Biol. 24, 370–376.
Kuhn, T.S., 1996. The Structure of Scientific Revolutions, 3rd ed. University of Chicago Press, Chicago.
Lee, J.Y., Cho, S.K., Sager, R., 2011. Plasmodesmata and non-cell-autonomous signaling in plants. In: Murphy, A.S., Peer, W., Schulz, B. (Eds.), The Plant Plasma Membrane (Plant Cell Monographs 19). Springer, Berlin, pp. 87–107.
Lew, R.R., 2005. Mass flow and pressure-driven hyphal extension in *Neurospora crassa*. Microbiology 151, 2685–2692.
Liesche, J., Gao, C., Binczycki, P., Andersen, S.R., Rademaker, H., Schulz, A., Martens, H. J., 2019. Direct comparison of leaf plasmodesma structure and function in relation to phloem-loading type. Plant Physiol. 179, 1768–1778.
Lim, W., Mayer, B., Pawson, T., 2015. Cell Signaling. Garland Science, New York.
López-Sáez, J.F., Giménez-Martín, G., Risueño, M.C., 1966. Fine structure of the plasmodesm. Protoplasma 61, 81–84.
Lucas, W.J., Lee, J.Y., 2004. Plasmodesmata as a supracellular control network in plants. Nat. Rev. Mol. Cell Biol. 5, 712–726.
Marchant, H.J., 1976. Plasmodesmata in algae and fungi. In: Gunning, B.E.S., Robards, A.W. (Eds.), Intercellular Communication in Plants: Studies on Plasmodesmata. Springer, Berlin, pp. 59–80.
Markham, P., 1994. Occlusions of septal pores in filamentous fungi. Mycol. Res. 98, 1089–1106.
Martens, H.J., Roberts, A.G., Oparka, K.J., Schulz, A., 2006. Quantification of plasmodesmatal endoplasmic reticulum coupling between sieve elements and companion cells using fluorescence redistribution after photobleaching. Plant Physiol. 142, 471–480.
McCaskill, A., Turgeon, R., 2007. Phloem loading in *Verbascum phoenicum* L. depends on the synthesis of raffinose-family oligosaccharides. Proc. Natl. Acad. Sci. U. S. A. 104, 19619–19624.
McLaughlin, S., 1989. The electrostatic properties of membranes. Annu. Rev. Biophys. Biophys. Chem. 18, 113–136.
Meeuse, A.D.J., 1957. Plasmodesmata (Vegetable Kingdom). Protoplasmatologia II.A.a.c. Springer, Wien.
Meşe, G., Richard, G., White, T.W., 2007. Gap junctions: basic structure and function. J. Invest. Dermatol. 127, 2516–2524.
Mohl, H., 1828. Ueber die Poren des Pflanzen-Zellgewebes. Heinrich Laupp, Tübingen.
Moor, H., 1987. Theory and practice of high pressure freezing. In: Steinbrecht, R.A., Zierold, K. (Eds.), Cryotechniques in Biological Electron Microscopy. Springer, Berlin, pp. 175–191.
Mullendore, D.L., Windt, C.W., van As, H., Knoblauch, M., 2010. Sieve tube geometry in relation to phloem flow. Plant Cell 22, 579–593.
Münch, E., 1930. Die Stoffbewegungen in der Pflanze. Gustav Fischer, Jena.
Nägeli, C., 1861. Ueber die Siebröhren von *Cucurbita*. Sitzungsber. Königl. Bayer. Akad. Wissens. 1861 (1), 212–238 (with tables I, II).
Neal, H.V., 1921. Nerve and plasmodesma. J. Comp. Neurol. 33, 65–75.
Nicholson, D.J., 2010. Biological atomism and cell theory. Stud. Hist. Philos. Biol. Biomed. Sci. 41, 202–211.

Nicolas, W.J., Grison, M.S., Trépout, S., Gaston, A., Fouché, M., Cordelières, F.P., Oparka, K., Tilsner, J., Brocard, L., Bayer, E.M., 2017. Architecture and permeability of post-cytokinesis plasmodesmata lacking cytoplasmic sleeves. Nat. Plants 3, 17082.
Nicolas, W.J., Grison, M.S., Bayer, E.M., 2018. Shaping intercellular channels of plasmodesmata: the structur-to-function missing link. J. Exp. Bot. 69, 91–103.
Oda, Y., Aoshima, A., 2002. Ab initio quantum chemical study on charge distribution and molecular structure of uranyl (VI) species with Raman frequency. J. Nucl. Sci. Technol. 39, 647–654.
Oparka, K.J., Boevink, P., 2005. Techniques for imaging intercellular transport. In: Oparka, K.J. (Ed.), Plasmodesmata. Blackwell Publishing, Oxford, pp. 241–262.
Oparka, K.J., Roberts, A.G., Boevink, P., Santa Cruz, S., Roberts, I., Pradel, K.S., Imlau, A., Kotlizky, G., Sauer, N., Epel, B., 1999. Simple, but nor branched, plasmodesmata allow the nonspecific trafficking of proteins in developing leaves. Cell 97, 743–754.
Otero, S., Helariutta, Y., Benitez-Alfonso, Y., 2016. Symplastic communication in organ formation and tissue patterning. Curr. Opin. Plant Biol. 29, 21–28.
Overall, R.L., Wolfe, J., Gunning, B.E.S., 1982. Intercellular communication in *Azolla* roots. I. Ultrastructure of plasmodesmata. Protoplasma 111, 134–150.
Petit, J.D., Li, Z.P., Nicolas, W.J., Grison, M.S., Bayer, E.M., 2020. Dare to change, the dynamics behind plasmodesmata-mediated cell-to-cell communication. Curr. Op. Plant Biol. 53, 80–89.
Pitzalis, N., Heinlein, M., 2017. The roles of membranes and associated cytoskeleton in plant virus replication and cell-to-cell movement. J. Exp. Bot. 69, 117–132.
Płachno, B.J., Świątek, P., 2011. Syncytia in plants: cell fusion in the endosperm–placental syncytium formation in *Utricularia* (Lentibulariaceae). Protoplasma 248, 425–435.
Plecis, A., Schoch, R.B., Renaud, P., 2005. Ionic transport phenomena in nanofluidics: experimental and theoretical study of the exclusion-enrichment effect on a chip. Nano Lett. 5, 1147–1155.
Ramirez, P., Cervera, J., Gomez, V., Ali, M., Nasir, S., Ensinger, W., Mafe, S., 2019. Membrane potential of single asymmetric nanopores: divalent cations and salt mixtures. J. Membr. Sci. 573, 579–587.
Ramírez-Weber, F.-A., Kornberg, T.B., 1999. Cytonemes: cellular processes that project to the principal signaling center in Drosophila imaginal discs. Cell 97, 599–607.
Ramón Cajal, S., 1908. Nouvelles observations sur l'évolution des neuroblastes, avec quelques remarques sur l'hypothése neurogénétique de Hensen-Held. Anat. Anz. 32 (1–25), 65–87.
Raven, J.A., 2005. Evolution of plasmodesmata. In: Oparka, K.J. (Ed.), Plasmodesmata. Blackwell Publishing, Oxford, pp. 33–52.
Raven, P.H., Evert, R.F., Eichhorn, S.E., 1999. Biology of Plants, 6th ed. W.H. Freeman: Worth Publishers, New York.
Reimer, L., Kohl, H., 2008. Transmission Electron Microscopy. Physics of Image Formation, 5th ed. Springer, Berlin.
Rennie, E.A., Turgeon, R., 2009. A comprehensive picture of phloem loading strategies. Proc. Natl. Acad. Sci. U. S. A. 106, 14162–14167.
Reynolds, A., 2010. The redoubtable cell. Stud. Hist. Philos. Biol. Biomed. Sci. 41, 194–201.
Reynolds, A.S., 2018. The Third Lens. Metaphor and the Creation of Modern Cell Biology. University of Chicago Press, Chicago.
Rice, C.L., Whitehead, R., 1965. Electrokinetic flow in a narrow cylindrical capillary. J. Phys. Chem. 69, 4017–4024.
Robards, A.W., 1968. Desmotubule – a plasmodesmatal substructure. Nature 218, 784.
Robards, A.W., 1976. Plasmodesmata in higher plants. In: Gunning, B.E.S., Robards, A. W. (Eds.), Intercellular Communication in Plants: Studies on Plasmodesmata. Springer, Berlin, pp. 15–57.
Robards, A.W., Lucas, W.J., Pitts, J.D., Jongsma, H.J., Spray, D.C. (Eds.), 1990. Parallels in Cell to Cell Junctions in Plants and Animals. Springer, Berlin.
Roberts, A.G., 2005. Plasmodesmal structure and development. In: Oparka, K.J. (Ed.), Plasmodesmata. Blackwell Publishing, Oxford, pp. 1–32.
Robinson-Beers, K., Evert, R.F., 1991. Fine structure of plasmodesmata in mature leaves of sugarcane. Planta 184, 307–318.
Ross-Elliott, T.J., Jensen, K.H., Haaning, K.S., Wager, B.M., Knoblauch, J., Howell, A.H., Mullendore, D.L., Moteith, A.G., Paultre, D., Yan, D., Otero, S., Bourdon, M., Sager, R., Lee, J.-Y., Helariutta, Y., Knoblauch, M., Oparka, K.J., 2017. Phloem unloading in Arabidopsis roots is convective and regulated by the phloem-pole pericycle. eLife 6, e24125.
Roth-Nebelsick, A., 2007. Computer-based studies of diffusion through stomata of different architecture. Ann. Bot. 100, 23–32.
Rouquerol, J., Avnir, D., Fairbridge, C.W., Everett, D.H., Haynes, J.H., Pernicone, N., Ramsay, J.D.F., Sing, K.S.W., Unger, K.K., 1994. Recommendations for the characterization of porous solids. Pure Appl. Chem. 66, 1739–1758.
Rustom, A., 2016. The missing link: does tunnelling nanotube-based supercellularity provide a new understanding of chronic and lifestyle diseases? Open Biol. 6, 160057.
Rutschow, H.L., Baskin, T.I., Kramer, E.M., 2011. Regulation of solute flux through plasmodesmata in the root meristem. Plant Physiol. 155, 1817–1826.
Schoch, R.B., Han, J., Renaud, P., 2008. Transport phenomena in nanofluidics. Rev. Mod. Phys. 80, 839–883.
Schuldiner, M., Schwappach, B., 2013. From rags to riches – the history of the endoplasmic reticulum. Biochim. Biophys. Acta 1833, 2389–2391.
Schulz, A., 1990. Conifers. In: Behnke, H.-D., Sjolund, R.D. (Eds.), Sieve Elements. Springer, Berlin, pp. 63–88.
Schulz, A., 1999. Physiological control of plasmodesmal gating. In: van Bel, A.J.E., van Kesteren, W.J.P. (Eds.), Plasmodesmata. Springer, Berlin, pp. 173–204.
Seybold, A., 1929. Die pflanzliche Transpiration. Ergebn. d. Biol. 5, 29–165.
Simon, M.L.A., Platre, M.P., Marquès-Bueno, M.M., Armengot, L., Stanislas, T., Bayle, V., Caillaud, M.-C., Jaillais, Y., 2016. A PtdIns(4)P-driven electrostatic field controls cell membrane identity and signalling in plants. Nat. Plants 2, 16089.
Singh, K.P., 2016. Ion current rectification influenced by length and location of surface charge in fluidic unipolar conical nanopores. Sens. Actuators B: Chem. 230, 493–500.
Sisakhtnezhad, S., Khosravi, L., 2015. Emerging physiological and pathological implications of tunneling nanotubes formation between cells. Eur. J. Cell Biol. 94, 429–443.
Skerrett, I.M., Williams, J.B., 2017. A structural and functional comparison of gap junction channels composed of connexins and innexins. Dev. Neurobiol. 77, 522–547.
Sparreboom, W., van den Berg, A., Eijkel, J.C.T., 2009. Principles and applications of nanofluidic transport. Nat. Nanotechnol. 4, 713–720.
Spiegelman, Z., Wu, S., Gallagher, K.L., 2019. A role for the endoplasmic reticulum in the cell-to-cell movement oft SHORT-ROOT. Protoplasma 256, 1455–1459.
Squires, T.M., Quake, S.R., 2005. Microfluidics: fluid physics at the nanoliter scale. Rev. Mod. Phys. 77, 977–1026.
Stadler, R., Lauterbach, C., Sauer, N., 2005. Cell-to-cell movement of green fluorescent protein reveals post-phloem transport in the outer integument and identifies symplastic domains in Arabidopsis seeds and embryos. Plant Physiol. 139, 701–712.
Strasburger, E., 1892. Schwärmsporen, Gameten, pflanzliche Spermatozoiden und das Wesen der Befruchtung. Histol. Beitr. 4, 48–156 (with Table III).
Strasburger, E., 1893. Ueber die Wirkungssphäre der Kerne und die Zellgrösse. Histol. Beitr. 5, 96–124.
Strasburger, E., 1901. Ueber Plasmaverbindungen pflanzlicher Zellen. Jahrb. wiss. Bot. 36, 493–610 (with Tables XIV, XV).
Tagliazucchi, M., Szleifer, I., 2015. Transport mechanisms in nanopores and nanochannels: can we mimic nature? Mat. Today 18, 131–142.
Taiz, L., Alkon, D., Draguhn, A., Murphy, A., Blatt, M., Hawes, C., Thiel, G., Robinson, D. G., 2019. Plants neither possess nor require consciousness. Trends Plant Sci. 24, 677–687.
Tajparast, M., Virdi, G., Glavinović, M.I., 2015. Spatial profiles of potential, ion concentration and flux in short unipolar and bipolar nanopores. Biochim. Biophys. Acta 1848, 2138–2153.
Tangl, E., 1880. Ueber offene Communicationen zwischen den Zellen des Endosperms einiger Samen. Jahrb. wiss. Bot. 12, 170–190 (with Tables IV–VI).
Ternetz, C., 1900. Protoplasmabewegung und Fruchtkörperbildung bei *Ascophanus carneus*. Jahrb. wiss. Bot. 35, 273–312 (with Table VII).
Terry, B.R., Robards, A.W., 1987. Hydrodynamic radius alone governs the mobility of molecules through plasmodesmata. Planta 171, 145–157.
Terry, B.R., Matthews, E.K., Haseloff, J., 1995. Molecular characterization of recombinant green fluorescent protein by fluorescence correlation microscopy. Biochem. Biophys. Res. Commun. 217, 21–27.
Thomas, J.A., McGaughey, A.J.H., 2009. Water flow in carbon nanotubes: transition to subcontinuum transport. Phys. Rev. Lett. 102, 184502.
Tilsner, J., Nicolas, W., Rosado, A., Bayer, E.M., 2016. Staying tight: plasmodesmal membrane contact sites and the control of cell-to-cell connectivity in plants. Annu. Rev. Plant Biol. 67, 337–364.
Ting, I.P., Loomis, W.E., 1963. Diffusion through stomates. Am. J. Bot. 50, 866–870.
Ting, I.P., Loomis, W.E., 1965. Further studies concerning stomatal diffusion. Plant Physiol. 40, 220–228.
van Bel, A.J.E., 2018. Plasmodesmata: a history of conceptual surprises. In: Sahi, V.P., Baluška, F. (Eds.), Concepts in Cell Biology - History and Evolution (Plant Cell Monographs 23). Springer, Berlin, pp. 221–270.
van Bel, A.J.E., Oparka, K.J., 1995. On the validity of plasmodesmograms. Bot. Acta 108, 174–182.
Velve-Casquillas, G., Le Berre, M., Piel, M., Tran, P.T., 2010. Microfluidic tools for cell biological research. Nano Today 5, 28–47.
Verweij, H., Schillo, M.C., Li, J., 2007. Fast mass transport through carbon nanotube membranes. Small 3, 1996–2004.
Vijayaraghavan, M.R., Prabhakar, K., 1984. The endosperm. In: Johri, B.M. (Ed.), Embryology of Angiosperms. Springer, Berlin, pp. 319–376.
Vogel, S., 1994. Life in Moving Fluids. The Physical Biology of Flow, 2nd ed. Princeton University Press, Princeton.
Wang, N., Fisher, D.B., 1994. The use of fluorescent tracers to characterize the post-phloem transport pathway in maternal tissues of developing wheat grains. Plant Physiol. 104, 17–27.
Weinstein, J.N., Blumenthal, R., Klausner, R.D., 1986. Carboxyfluorescein leakage assay for lipoprotein-liposome interaction. Meth. Enzymol. 128, 657–668.
Wu, S., Gallagher, K.L., 2011. Mobile protein signals in plant development. Curr. Opin. Plant Biol. 14, 563–570.
Yan, D., Liu, Y., 2020. Diverse regulation of plasmodesmal architecture facilitates adaptation to phloem translocation. J. Exp. Bot. 71, 2505–2512.
Zavaliev, R., Ueki, S., Epel, B.L., Citovsky, V., 2011. Biology of callose (β-1,3-glucan) turnover at plasmodesmata. Protoplasma 248, 117–130.
Zhang, C., Scholpp, S., 2019. Cytonemes in development. Curr. Opin. Gen. Dev. 58, 25–30.
Zhong, Q., Ding, H., Gao, B., He, Z., Gu, Z., 2019. Advances of microfluidics in biomedical engineering. Adv. Mater. Technol. 4, 1800663.
Zwienicki, M.A., Haaning, K.S., Boyce, C.K., Jensen, K.H., 2016. Stomatal design principles in synthetic and real leaves. Interface 13, 20160535.